


**OPEN ACCESS**

EDITED BY  
 Matthew Collins,  
 University of Exeter, United Kingdom

REVIEWED BY  
 Houssam Ayt Ougougdal,  
 Cadi Ayyad University, Morocco  
 Rusmawan Suwarman,  
 Bandung Institute of Technology,  
 Indonesia

\*CORRESPONDENCE  
 Adhi Harmoko Saputro  
 ✉ adhi@sci.ui.ac.id

RECEIVED 18 November 2025  
 REVISED 19 January 2026  
 ACCEPTED 27 January 2026  
 PUBLISHED 23 February 2026

CITATION  
 Prasetya R, Djuhana D, Saputro AH and  
 Permana DS (2026) Evaluation and  
 ranking of NEX-GDDP-CMIP6 models  
 based on monthly precipitation  
 climatology over Indonesia.  
*Front. Clim.* 8:1748663.  
 doi: 10.3389/fclim.2026.1748663

COPYRIGHT  
 © 2026 Prasetya, Djuhana, Saputro and  
 Permana. This is an open-access article  
 distributed under the terms of the  
[Creative Commons Attribution License  
 \(CC BY\)](https://creativecommons.org/licenses/by/4.0/). The use, distribution or  
 reproduction in other forums is  
 permitted, provided the original  
 author(s) and the copyright owner(s) are  
 credited and that the original publication  
 in this journal is cited, in accordance  
 with accepted academic practice. No  
 use, distribution or reproduction is  
 permitted which does not comply with  
 these terms.

# Evaluation and ranking of NEX-GDDP-CMIP6 models based on monthly precipitation climatology over Indonesia

Ratih Prasetya<sup>1,2</sup>, Dede Djuhana<sup>1</sup>, Adhi Harmoko Saputro<sup>1\*</sup> and Donaldi Sukma Permana<sup>2</sup>

<sup>1</sup>Department of Physics, Faculty of Mathematics and Natural Sciences, Universitas Indonesia, Depok, Indonesia, <sup>2</sup>Indonesian Agency for Meteorology Climatology and Geophysics, Jakarta, Indonesia

**Introduction:** As a tropical archipelago, Indonesia is exceptionally susceptible to climate change impacts. Since mitigation requires accurate regional climate data, a reliable model assessment is essential to address the biases and uncertainties of Global Climate Model's (GCMs). This study evaluates and ranks 35 NASA NEX-GDDP-CMIP6 models, including their multi-model mean ensemble (ENSMEAN), on their capacity to simulate monthly precipitation climatology over Indonesia.

**Methods:** The methodology employed MSWEP dataset as the observational reference, utilizing statistical metrics including Correlation Coefficient (CC), Normalized Standard Deviation (NSTD), Root Mean Square Deviation (RMSD) and Mean Bias (MB). A dual-scale evaluation framework was adopted, assessing the model's spatio-temporal performance. Taylor Diagrams used to visualize model distribution, while Min-Max normalization and the Summation of Rank (SR) applied to ensure fair comparison and identify the best-performing models.

**Discussion:** The findings demonstrate that NEX-GDDP-CMIP6 models generally capture Indonesia's seasonal precipitation patterns in close alignment with MSWEP observations. Notably, five models that consistently identified as high performers across spatio-temporal dimensions were ACCESS-CM2, CMCC-ESM2, TaiESM1, MRI-ESM2-0 and CESM2-WACCM. Specifically, ACCESS-CM2 showed the highest temporal accuracy, while TaiESM1 demonstrated the strongest spatial accuracy. ENSMEAN ranked seventh across spatio-temporal dimensions, proving its capability of reducing errors and enhancing simulation reliability. Despite the model's overall accuracy, systematic biases persists, such as a "February dip" that underestimates peak wet-season precipitation and a tendency to overestimate precipitation during the dry season. These discrepancies suggests that simulating precipitation interactions among monsoon dynamics, topography and land-sea contrast remain challenging in Indonesia Maritime Continent. This study offers a benchmark for GCMs selection and underscores the need for improved regional models to support climate adaptation and hydrological policymaking.

**KEYWORDS**

climate change, GCM evaluation, Indonesia, monthly climatology, precipitation

## 1 Introduction

Anthropogenic greenhouse gas emissions act as primary drivers of global warming (Ngai et al., 2022). This leads to climate extremes with significant impacts in ecosystem (Lungarska and Chakir, 2024), infrastructures (Iradukunda et al., 2024) and humans (Irwandi et al., 2021). Recent studies projected that Southeast Asian surface temperatures could rise by over 3.5 °C by 2,100 (Raghavan et al., 2018). Developing countries in Southeast Asia may face severe climate change impacts, including Indonesia (Francisco et al., 2006). Indonesia undergoes significant flood risk due to heavy precipitation (Qian, 2008). As a tropical archipelago, this region also highly susceptible to climate extremes (Griffiths et al., 2013). Therefore, long-term climate simulations are essential for adaptation in tropical monsoonal regions (Vicente-Serrano et al., 2022). Global Climate Model's (GCMs) are widely used for past and future climate simulations due to their extensive application in climate studies (Chen et al., 2021; Pereira et al., 2023).

Coupled Model Intercomparison Project (CMIP) provides widely used GCMs that integrate coupled models of atmosphere, ocean, land surface, and sea ice components (Meehl et al., 2004). CMIP Phase 6 (CMIP6) facilitates the study of climate change widely (Soumya, 2025). However, many CMIP6 models exhibit regional precipitation biases and uncertainties (Dahiya et al., 2024; Konda and Vissa, 2022). Whereas, some models tend to show superior skill in precipitation simulation compared to others (Mohammed, 2025). For example, MRI-ESM2-0, EC-Earth3, and EC-Earth3-Veg were identified as the most proper models for future precipitation over the Southeast Asia continent (Iqbal et al., 2020). EC-Earth, GFDL, and NorESM also demonstrate superior skill in simulating seasonal precipitation over the Pacific and East Asia (Chen et al., 2021). Additionally, CMCC-CM2-SR5, CNRM-CM6-1, MIROC-ES2L, IPSL-CM6A-LR, and INM-CM5-0 best capture precipitation and drought projections in Pakistan (Shakeel et al., 2025). The top multi-model ensembles to simulate precipitation over Southeast Asia were identified to be EC-Earth3, EC-Earth3-Veg, and E3SM-1-0 (Liu et al., 2023). While CMIP6 captures global climate complexity, its precipitation simulations are limited by coarse spatial resolution (Chen et al., 2021).

NASA Earth Exchange Global Daily Downscaled Projections (NEX-GDDP-CMIP6) dataset provides downscaled projections that offer superior regional detail compared to standard GCMs (Bao and Wen, 2017). The dataset facilitates finer-scale precipitation modeling across topographical features (Jiang et al., 2023). Studies show NEX-GDDP-CMIP6 improves upon CMIP6 in capturing extreme precipitation over the India (Kumar et al., 2020), Ireland (Moradian et al., 2024), China (Yuan et al., 2024), Southeast Asia (Raghavan et al., 2018) and Africa (Musie et al., 2020). However, this high-resolution GCM's remains underutilized for studying long-term precipitation patterns across Indonesia. While the NEX-GDDP-CMIP6 provides significant advancement in climate modeling, the large spread among individual models introduces uncertainty for regional applications (Thrasher et al., 2022). Further study into the dataset's multi-model mean ensemble (ENSMEAN) is necessary to enhance simulation accuracy as suggested by Baghel et al. (2022). In a complex archipelago such as Indonesia, where systematic evaluations of GCM's are still limited, objective evaluation ranking is essential (Kurniadi et al., 2023). Therefore, this study proposes to evaluate and rank NEX-GDDP-CMIP6 model along with its ENSMEAN to identify the best suitable climate models in Indonesia. This ranking provides a benchmark for identifying a subset of models, thereby minimizing

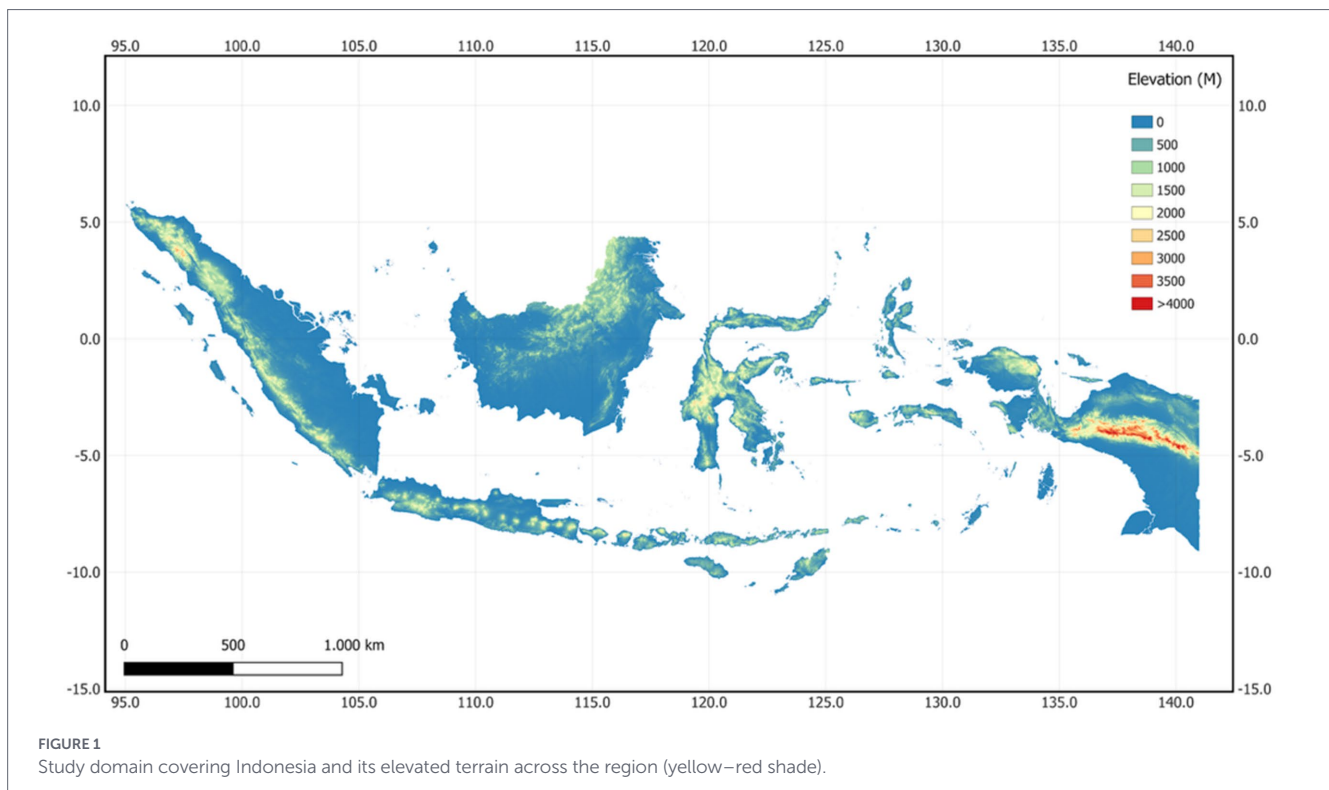
uncertainties and ensuring that adaptation strategies are based on the most reliable model's simulations.

The specific aims of this study were to: (a) evaluate and rank the performance of NEX-GDDP-CMIP6 models over Indonesia using monthly mean climatological analysis against the Multi-Source Weighted-Ensemble Precipitation (MSWEP) reference dataset, (b) propose the five best-performing models for spatio-temporal precipitation analysis, and (c) investigate Indonesia climatic patterns as represented by the best-performing models. The consideration of Indonesia as a climate-sensitive region shows the need for further analysis using recent models. Consequently, finding of this study are expected to provide scientific insight into the robustness of the multi-metric ranking method. Further, offer guidance for selecting appropriate NEX-GDDP-CMIP6 models for Indonesia. This study facilitates climate change adaptation planning and informs policy decisions to support sustainable development. The next sections include the detailed information on the Indonesia region in the "Study Area" section, "Materials and Methods" focuses on the dataset and study workflow, "Results" and "Discussion" presents comprehensive statistical results, while "Conclusion" provides the summary of results and recommendations for future studies.

## 2 Study area

The domain of this study is the Indonesian region as depicted in Figure 1, the largest world archipelagic country (Griffiths et al., 2013). Indonesia, which is located between Asia and Australia, lies between the Pacific and Indian Oceans. It has a vast and intricate territory comprising of 17,000 islands (Lee, 2015). It geographically covers a region of 6° 08' North Latitude - 11° 15' South Latitude and 95°-141° East Longitude, with a longitude of 5,000 km or 1/8 of the equatorial landscape. The land area is approximately 10,000,000 km<sup>2</sup> with a 2,720,000 km<sup>2</sup> sea-land ratio of 2.7:7.3 which is close to the 3:7 recorded for the surface of the Earth (Yamanaka, 2016). Indonesia has major islands of Sumatra, Java, Kalimantan, Sulawesi, and Papua with several other small islands, while approximately 70% of the territory is covered by ocean (Mahiru Rizal et al., 2019). The focus of this study is on the continent of Indonesia, whereas the neighboring countries such as Malaysia close to Borneo, Papua New Guinea close to New Guinea, Timor-Leste close to Timor, and all the surrounding oceanic areas are excluded through spatial masking.

Located in tropics, Indonesia experiences hot and humid climate throughout the year (Chang et al., 2004). The country shows a distinct seasonal cycle of Asia-Australian monsoon (Robertson et al., 2011; Wheeler and McBride, 2007). Its monsoonal system cycle includes wet season from October to March and the dry season from April to September (Ramage, 1971). This is associated with the westerly winds and El Niño—Southern Oscillation (ENSO) influencing the climate of the country as well as the ocean warming which increases the amount of precipitation in some regions (Lee, 2015; Yamanaka, 2016). Notably, the monsoon timing has increasingly become variable due to climate change (Adriat et al., 2025). The Madden-Julian Oscillation (MJO) shows significant equatorial variability over the region (Tang and Yu, 2008). Thus, modulates precipitation across Indonesia (Lubis et al., 2022). The country precipitation anomalies also strongly influenced by El Niño and Indian Ocean Dipole mode (IOD) (Nur'utami and Hidayat, 2016). Moreover, precipitation characteristic in



Indonesia is reported non-stationary, with a central–eastern increase and a central–western decrease (Sudarman et al., 2024). Regional dynamics in Indonesia can be examined using GCM’s numerical simulations, despite their coarse resolutions (Ferijal et al., 2025). This trend highlights the need for further study using the latest GCM to improve the precision and spatial detail of precipitation simulations.

## 3 Materials and methods

### 3.1 Climate model dataset

The NEX-GDDP-CMIP6 developed by NASA as an improvement of CMIP6. The dataset offers 35 models with  $0.25^\circ$  spatial resolution (approximately 25 km) to provide finer details than the original CMIP6 models that have native resolution typically around 100 km or coarser (Thrasher et al., 2022). The data archive contains downscaled 1950–2,100 historical and future projections that can be accessed from the website of NASA at <https://www.nccs.nasa.gov/services/data-collections/land-based-products/nex-gddp-cmip6>. NEX-GDDP-CMIP6 utilizes a daily variant of the monthly Bias Correction/Spatial Disaggregation (BCSD) algorithm for its statistical downscaling. BCSD corrects and downscales CMIP6 data to bridge the gap in coarse-scale model outputs (Jain et al., 2019). BCSD method employs in two steps. First, quantile mapping bias correction used to align GCM’s distributions with historical observations, removing systematic errors. Second, spatial disaggregation interpolates into  $0.25^\circ$  grid for improved spatial resolution.

This study used the daily temporal resolution of NEX-GDDP-CMIP6 precipitation dataset with the historical period of 1985 to 2014, accessed in September 2023. The dataset includes all historical simulations of 35 NEX-GDDP-CMIP6 models as shown in Table 1.

Variant of the models identified by code specifying key attributes given by letter and number of rNiNpNfN including realization index, initialization method, parameterization, and forcing variant (Moradian et al., 2023). The realization (r) stands for certain running simulation, the initialization (i) stands for initial conditions, and the physics (p) stands for the model physics version. The forcing (f) denotes the version of forcing index employed. The variant r1i1p1f1 represents the first version of realization, first version of initialization, first version of physics and first forcing index simulation (Gummadi et al., 2025). These simulations offer a reliable basis for studying precipitation dynamics, climate impacts and adaptation.

ENSMEAN, in this study, employed to reduce the uncertainty and variability of individual models to a certain degree (Guo et al., 2023; Nwokolo et al., 2023). ENSMEAN model was generated after land-sea masking step by calculating the unweighted ensemble mean of monthly climatological output from 35 NEX-GDDP-CMIP6 models. An unweighted (simple) average was chosen for its simplicity and as a robust baseline for comparison. This approach does not account for the varying skill/performance of individual models, which a performance-based or competence-weighted ensemble would address.

### 3.2 Observational dataset

The limitations of long-term observational records in Indonesia led to the adoption of the MSWEP (v2), which covered 1985–2014 of daily temporal and  $0.1^\circ$  spatial resolution in this study. The MSWEP was used as the observational reference against the NEX-GDDP-CMIP6. The dataset covers 1979 up to the present day (Beck et al., 2017) and has  $0.1^\circ$  spatial resolution. The MSWEP exemplifies systematic data merging by assimilating the strengths of satellite, gauge, and reanalysis-based daily precipitation estimates. The adoption of the dataset in this study was based on the detailed information presented by Beck et al. (2019). The

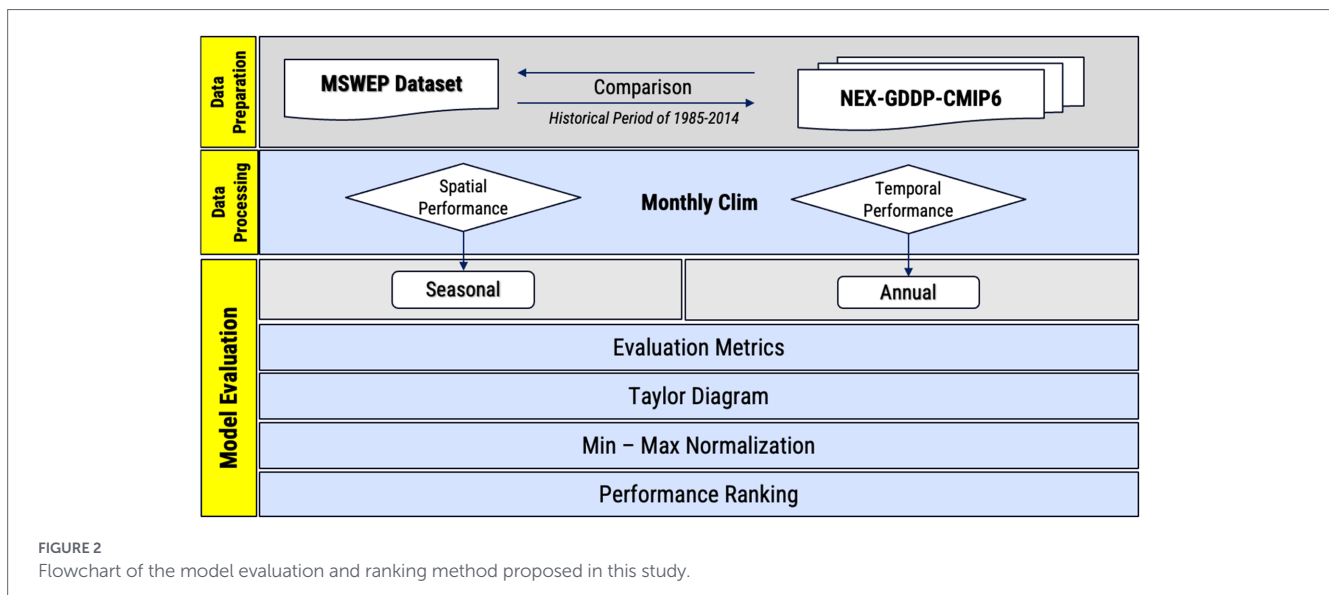
TABLE 1 List of climate models compared with the MSWEP dataset.

Specifications	Model's name	Variant
Model	1. ACCESS-CM2: Commonwealth Scientific and Industrial Research Organization, Australia (Bi et al., 2020)	r1i1p1f1
	2. ACCESS-ESM1-5: Commonwealth Scientific and Industrial Research Organization, Australia (Ziehn et al., 2020)	r1i1p1f1
	3. BCC-CSM2-MR: Beijing Climate Center, China Meteorological Administration, China (Wu et al., 2019)	r1i1p1f1
	4. CanESM5: Canadian Centre for Climate Modeling and Analysis, Canada	r1i1p1f1
	5. CESM2: National Center for Atmospheric Research, USA (Swart et al., 2019)	r4i1p1f1
	6. CESM2-WACCM: National Center for Atmospheric Research, USA (Danabasoglu et al., 2020)	r3i1p1f1
	7. CMCC-CM2-SR5: Fondazione Centro Euro-Mediterraneo sui Cambiamenti Climatici, Italy (Cherchi et al., 2019)	r1i1p1f1
	8. CMCC-ESM2: Fondazione Centro Euro-Mediterraneo sui Cambiamenti Climatici, Italy (Lovato et al., 2022)	r1i1p1f1
	9. CNRM-CM6-1: National Center of Meteorological Research, France (Voldoire et al., 2019)	r1i1p1f2
	10. CNRM-ESM2-1: National Center of Meteorological Research, France	r1i1p1f2
	11. EC-Earth3: EC-EARTH-CONSORTIUM, Europe (Séférian et al., 2019)	r1i1p1f1
	12. EC-Earth3-Veg-LR: EC-EARTH-CONSORTIUM, Europe (Döscher et al., 2022)	r1i1p1f1
	13. FGOALS-g3: Institute of Atmospheric Physics, Chinese Academy of Sciences, China (Pu et al., 2020)	r3i1p1f1
	14. GFDL-CM4: NOAA Geophysical Fluid Dynamics Laboratory, USA (Held et al., 2019)	r1i1p1f1
	15. GFDL-CM4-gr2: NOAA Geophysical Fluid Dynamics Laboratory, USA (Held et al., 2019)	r1i1p1f1
	16. GFDL-ESM4: NOAA Geophysical Fluid Dynamics Laboratory, USA (Dunne et al., 2020)	r1i1p1f1
	17. GISS-E2-1-G: Goddard Institute for Space Studies, USA (Kelley et al., 2020)	r1i1p1f2
	18. HadGEM3-GC31-LL: Met Office Hadley Centre, UK (Kuhlbrodt et al., 2018)	r1i1p1f3
	19. HadGEM3-GC31-MM: Met Office Hadley Centre, UK	r1i1p1f3
	20. IITM-ESM: Indian Institute of Tropical Meteorology, India (Kuhlbrodt et al., 2018)a	r1i1p1f1
	21. INM-CM4-8: Institute for Numerical Mathematics, Russia (E. M. Volodin et al., 2018)	r1i1p1f1
	22. INM-CM5-0: Institute for Numerical Mathematics, Russia (E. Volodin and Gritsun, 2018)	r1i1p1f1
	23. IPSL-CM6A-LR: Institute Pierre Simon Laplace, France (Boucher et al., 2020)	r1i1p1f1
	24. KACE-1-0-G: National Institute of Meteorological Sciences/ Korea Meteorological Administration, Republic of Korea (Pak et al., 2021)	r1i1p1f1
	25. KIOST-ESM: KIOST, Republic of Korea (Pak et al., 2021)	r1i1p1f1
	26. MIROC-ES2L: Japan Agency for Marine- Earth Science and Technology, Japan (Hajima et al., 2020)	r1i1p1f2
	27. MIROC6: Japan Agency for Marine- Earth Science and Technology, Japan (Tatebe et al., 2019)	r1i1p1f1
	28. MPI-ESM1-2-HR: Meteorological Research Institute, Japan (Müller et al., 2018)	r1i1p1f1
	29. MPI-ESM1-2-LR: Meteorological Research Institute, Japan (Mauritsen et al., 2019)	r1i1p1f1
	30. MRI-ESM2-0: Meteorological Research Institute, Japan (Yukimoto et al., 2019)	r1i1p1f1
	31. NESM3: Nanjing University of Information Science and Technology (NUIST), China (Cao et al., 2018)	r1i1p1f1
	32. NorESM2-LM: Norwegian Climate Service Centre, Norway (Seland et al., 2020)	r1i1p1f1
	33. NorESM2-MM: Norwegian Climate Service Centre, Norway (Seland et al., 2020)	r1i1p1f1
	34. TaiESM1: Research Center for Environmental Changes, Academia Sinica, Taiwan (Wang et al., 2021)	r1i1p1f1
	35. UKESM1-0-LL: UK Met Office Hadley Center, UKPSL-CM6A-LR: Institute Pierre Simon Laplace, France (Sellar et al., 2020)	r1i1p1f2
Simulation	Historical (1985–2014)	
Variable	pr	
Temporal Resolution	Daily	
Spatial Resolution	0.25° × 0.25°	

MSWEP provides high spatial resolution of 0.1° and up to 3-hourly temporal resolution considered well-suited for regional hydroclimate studies (Nazarian et al., 2024). The dataset is a reliable source of gridded precipitation data for climatological and hydrological studies related to Indonesia (Ferijal et al., 2025).

### 3.3 Methods

35 NEX-GDDP-CMIP6 and ENSMEAN model employed to conduct statistical evaluation in this study. The precipitation dataset was assessed against the MSWEP for the historical period of 1985–2014



(Lakew, 2020). Monthly mean climatology was calculated for both datasets to establish a baseline for comparison (Lee et al., 2013). Spatial performance was examined through seasonal climatological means of December–January–February (DJF), March–April–May (MAM), June–July–August (JJA), and September–October–November (SON). Temporal performance was analyzed using the annual climatological cycle as shown in Figure 2.

This dual scale evaluation framework of seasonal for spatial analysis and monthly for temporal analysis is based on the physical drivers of Indonesia. Spatial evaluation is conducted on a seasonal basis to capture monsoon-driven migration of Intertropical Convergence Zone (ITCZ) that affected precipitation distribution across Indonesia archipelago (Aldrian and Dwi Susanto, 2003). Temporal evaluation utilizes monthly data to assess the model's ability in simulating annual cycle. Specifically, temporal evaluation use in capturing the timing and magnitude of wet-dry months transitions which are critical to agricultural adaptation (Jun-Ichi et al., 2002). By evaluating spatio-temporal dynamics, this study ensure that the model ranking reflect the ability to simulate Indonesia's unique seasonal geography and monthly transitions of precipitation cycles.

The initial calculation was the adoption of the daily precipitation data to determine the monthly average with the aim of ensuring consistency. For each month  $m$  in year  $y$ , the monthly mean precipitation  $P_{m,y}$  was computed for all daily precipitation values.  $P_{(d,m,y)}$  represents the daily precipitation on the day  $d$  and  $n_{m,y}$  is the number of days in the month. Therefore, the monthly mean precipitation was determined using the following equation:

$$P_{m,y} = \frac{1}{n_{m,y}} \sum_{d=1}^{n_{m,y}} P_{(d,m,y)} \quad (1)$$

Equation (1) was used to calculate 30-year climatological monthly mean by averaging all months in the period. For a given month  $m$ , the climatological monthly mean was determined in Equation (2):

$$\bar{P}_m = \frac{1}{M} \sum_{y=1}^n P_{m,y} \quad (2)$$

$M = 30$  which is the total number of years and the Equation (2) produces long-term monthly climatology to represent the typical precipitation characteristics in a month. Furthermore, the annual climatology was computed by calculating the annual mean precipitation in each year. The annual mean for year  $y$  was determined based on the 12 monthly means as shown in Equation (3):

$$\bar{P}_y^{annual} = \frac{1}{12} \sum_{m=1}^{12} P_{m,y} \quad (3)$$

The 30-year climatology annual mean was subsequently obtained by averaging the annual means across the period. This was achieved using Equation (4):

$$\bar{P}^{annual} = \frac{1}{M} \sum_{y=1}^N P_y^{annual} \quad (4)$$

The performance of the models was quantified using statistical metrics for the purpose of detecting systematic deviations. The metrics used were Correlation Coefficient (CC), Normalized Standard Deviation (NSTD), and Mean Bias (MB) (Ngo-Duc et al., 2024). The Root Mean Standard Deviation (RMSD) evaluation metrics used in the Taylor plot were also adopted (Liu et al., 2024). Taylor diagrams were applied to show the combination of CC, NSTD, and RMSD that demonstrated the ability of each model to reproduce the variability observed. The adoption of Taylor diagram was associated with its advantages in evaluating model performance by simultaneously showing the correlation, variability, and errors in a single framework (Simão et al., 2020). The dataset were processed in Python programming language using a specific module of the Open Climate Workbench (OCW) (H. Lee et al., 2018). In addition, SkillMetrics (<https://pypi.org/project/SkillMetrics/1.1.3/>) and Matplotlib 3.2.2 libraries also employed in data processing. The steps for NEX-GDDP-CMIP6 and MSWEP included spatial cropping and land-sea masking over Indonesia. The observational MSWEP dataset was re-gridded to 0.25° NEX-GDDP grid to ensure a grid-to-grid comparison at daily time step. Following these

steps, evaluation metrics were calculated to assess model performance as provided in Table 1.

Specifically, MSWEP was used as the reference precipitation dataset  $R_i$  and the NEX-GDDP-CMIP6 as simulated precipitation  $S_i$ . Both were used to determine the average of the reference dataset and simulated precipitation, evaluated over 30 years. The average simulations and observations were provided as  $\bar{S}$  and  $\bar{R}$ . Furthermore, the variable  $N$  used in the metric computation formula is defined differently for each evaluation scale. For the spatial (seasonal mean) evaluation,  $N$  is the total number of grid cells across the domain (as the comparison is grid-to-grid on a single seasonal mean field). For the temporal (monthly climatology) evaluation,  $N$  is the total number of grid cells multiplied by the number of months in the annual cycle (12 months), as the long-term monthly climatology is compared across the whole domain.

The formula for each metric is presented in the following equation:

Correlation Coefficient (CC), in Equation (5), was used to evaluate the magnitude and orientation of the linear relationship between  $R_i$  and  $S_i$ :

$$CC = \frac{\sum_{i=1}^N (S_i - \bar{S})(R_i - \bar{R})}{\sqrt{\sum_{i=1}^N (S_i - \bar{S})^2} \sqrt{\sum_{i=1}^N (R_i - \bar{R})^2}} \quad (5)$$

Normalized Standard Deviation (NSTD) was used to determine the variability differences between  $R_i$  and  $S_i$  through the ratio of standard deviation as shown in Equation (6):

$$NSTD = \frac{\sigma_{S_i}}{\sigma_{R_i}} \quad (6)$$

NSTD was employed to assess variability differences between the simulations of  $S_i$  and the reference data of  $R_i$  by calculating the ratio of their standard deviation. This metric provides a dimensionless measure of relative variability. NSTD value close to 1 indicates that the simulations variability is comparable to the reference. Values higher or lower than unity represent overestimation or underestimation of the precipitation spread, respectively (Taylor, 2001).

Root Mean Standard Deviation (RMSD) evaluates the average deviation between  $R_i$  and  $S_i$  values, combining both systematic and random errors, as given in Equation (7):

$$RMSD = \sqrt{\frac{1}{N} \sum_{i=1}^N (S_i - R_i)^2} \quad (7)$$

Mean Bias (MB) was applied to measure the average deviations between  $R_i$  and  $S_i$  values in Equation (8). This was used to determine when a model over- or underestimated.

$$MB = \frac{1}{N} \sum_{i=1}^N (S_i - R_i) \quad (8)$$

### 3.3.1 Taylor diagram

The performance of the models was presented through the Taylor diagram (Taylor, 2001). It served as a standard graphical method for assessing the correspondence between model outputs and observational data (Achutarao et al., 2004; Gates et al., 1999). Taylor diagram offered a clear visualization of skills presented by the models. It allowed the assessment of the agreements and discrepancies with observations using three key metrics including RMSD, CC, and NSTD. The performance of NEX-GDDP-CMIP6 models and ENSMEAN in simulating monthly mean climatology was evaluated against the MSWEP using the Taylor diagram.

### 3.3.2 Metrics conversion and min-max normalization

The chosen statistical measures (CC, NSTD, RMSD and MB) were selected as a comprehensive set to cover different aspects of model skill, encompassing correlation, variability, total error and systematic bias. Since each calculated values of CC, NSTD, RMSD and MB has a different range, a conversion was performed to standardized them into uniform range of  $-\infty$  to 0 for the model ranking process. Consequently, a new set of metrics was defined through conversion to ensure comparability (Ngo-Duc et al., 2024). The conversion metrics calculations are given by following formula:

$$r_{CC} = CC - 1 \quad (9)$$

$$r_{NSTD} = -|NSTD - 1| \quad (10)$$

$$r_{RMSD} = -RMSD \quad (11)$$

$$r_{MB} = -|MB| \quad (12)$$

Where  $r$  represents the original value of the data point, with  $r_{CC}$  is the value conversion of Correlation Coefficient as given in Equation (9),  $r_{NSTD}$  is the value conversion of Normalized Standard Deviation as given in Equation (10),  $r_{RMSD}$  is the value conversion of Root Mean Standard Deviation as given in Equation (11), and  $r_{MB}$  is the value conversion of Mean Bias as given in Equation (12).

The best performing models are identified by  $r_{CC}$  and  $r_{NSTD}$  values close to 1. This referring the high degree of correlation and comparable variability with the reference data. For  $r_{RMSD}$ , the best performer of model is indicated with the lowest value.  $r_{MB}$ , the positive value ( $>0$ ) means the model has a “wet bias” (it overestimates precipitation). Whereas the negative value ( $<0$ ) indicated that the model has a “dry bias” (it underestimates precipitation).

Min-Max Normalization was then applied to transform new metrics with different ranges and units onto a uniform, comparable scale (0–1). This transformation is essential for ensuring a fair comparison across all performance criteria. Min–Max normalization applied to rescale all values because the metrics had different scales and units (Sarala, 2024). Equation (13) was used in the climate change studies, allowing for a consistent and uniform comparison of the data value. Equation (13) was applied to each data point to perform the transformation.

$$r_{norm} = \frac{r - r_{min}}{r_{max} - r_{min}} \tag{13}$$

$r_{min}$  is the minimum value,  $r_{max}$  stands for maximum value, and  $r_{norm}$  is the normalized value. The application was to ensure that higher normalized total scores consistently represented equal weighting of all models.

### 3.3.3 Summation of rank (SR)

In this study, the models were ranked using the Summation of Rank (SR) method. This method aggregated and quantified the overall scores across multiple metrics (Wati et al., 2022). The final summation of Rank (SR) was employed as a non-parametric and multi-criteria decision-making method that aggregates performance across all normalized metrics equally to identify the models with the most consistent overall skill.

This ranking method aimed to identify the top five models with the most robust performance (Chen et al., 2011; Chhin and Yoden, 2018). Specifically, in capturing seasonal and temporal precipitation relative to MSWEP across the region. The model with the higher  $R_{Total}$  is typically considered the best-performing because the total normalized score is higher across all metrics, as shown in Equation (14):

$$R_{Total} = r_{CC\_norm} + r_{NSTD\_norm} + r_{RMSD\_norm} + r_{MB\_norm} \tag{14}$$

Where  $r_{CC\_norm}$  is the normalized value of CC,  $r_{NSTD\_norm}$  is the normalized value of NSTD,  $r_{RMSD\_norm}$  is the normalized value of RMSD and  $r_{MB\_norm}$  is the normalized value of MB.

The final ranking utilizes the normalized score (ranging from 0 to 1) for calculating the total performance score,  $R_{Total}$ , not the ordinal rank. Min-Max normalization is designed to handle the ‘direction’ of the metrics by ensuring that for all metrics, including error metrics like RMSD and MB, a higher normalized value consistently indicates better performance. The total score is defined as the sum of the normalized scores  $R_{Total}$  as given in Equation 14. The final rank  $r$  is then determined as the ordinal rank based on this  $R_{Total}$  value, where the highest  $R_{Total}$  corresponds to Rank 1.

In this study, spatio-temporal evaluation was performed. The models were ranked according to the aggregated normalized scores of the four metrics with a maximum attainable score of 4. The spatial aspect was evaluated using seasonal data of DJF, MAM, JJA, and SON with the model rankings determined from the cumulative scores across the four metrics. Maximum attainable score is 16, derived from four seasonal scores per metric for each model. Subsequently, the temporal evaluation was conducted using monthly data across the four metrics with a maximum score of 4 per model. The equal weighting scheme that applied to all metrics, assuming that the model’s ability to replicate the mean bias (MB) state, error magnitude (RMSE), linear association (CC) and variability (NSTD) are of equal importance for regional climate assessment. This weighing avoids subjective bias by not favoring one statistical attribute over another (Rupp et al., 2013).

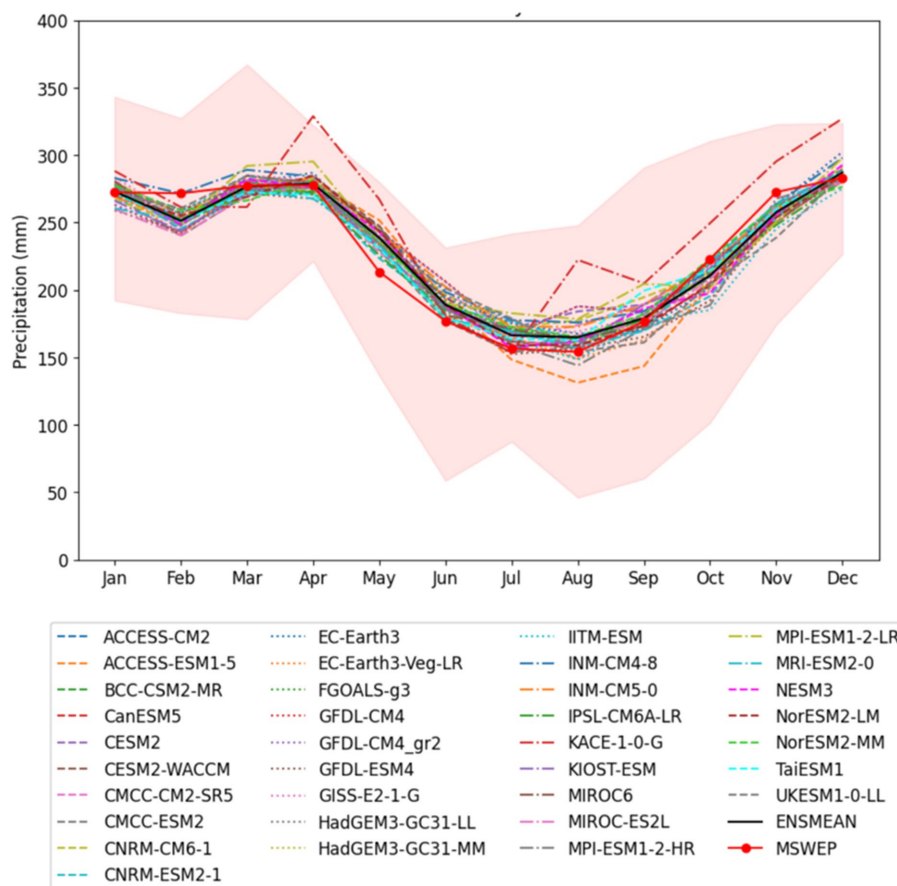
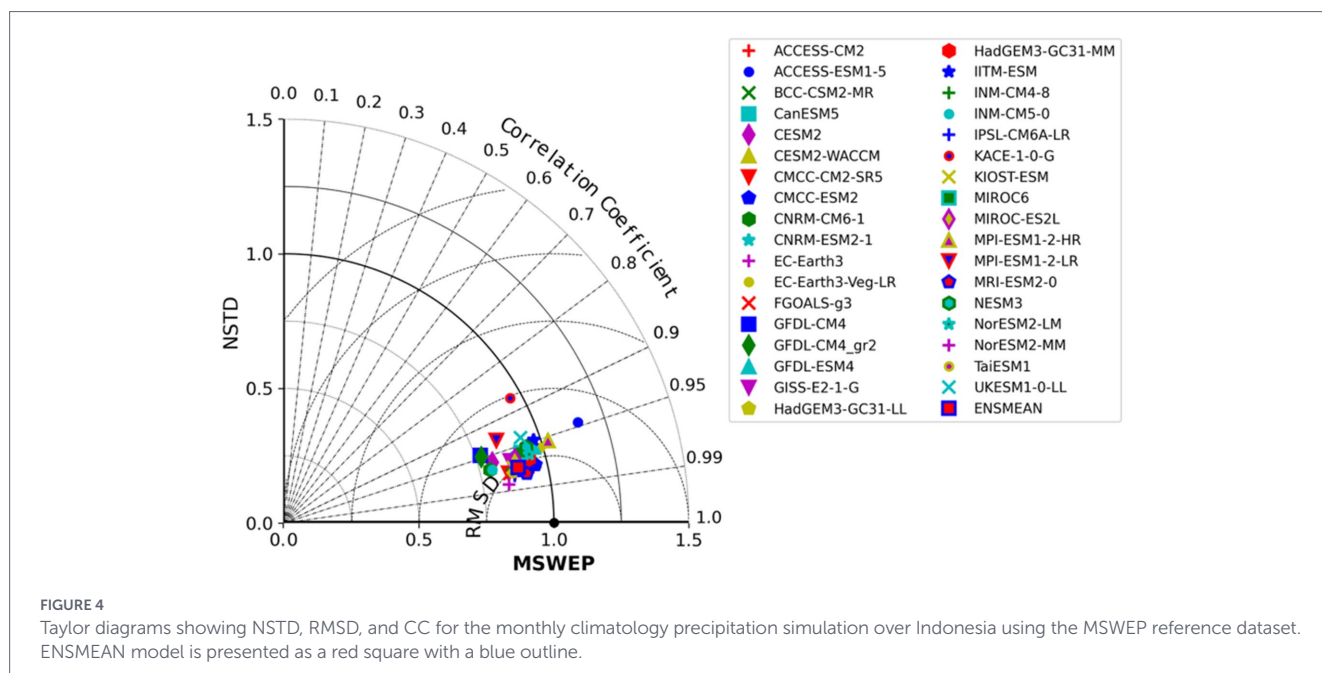


FIGURE 3 The seasonal precipitation cycle across the Indonesian region derived from 35 climate simulations, ENSMEAN, and the MSWEP reference dataset. The shaded pink area shows the full range of simulated outputs from all models which reflect the level of uncertainty.



**FIGURE 4**  
Taylor diagrams showing NSTD, RMSD, and CC for the monthly climatology precipitation simulation over Indonesia using the MSWEP reference dataset. ENSMEAN model is presented as a red square with a blue outline.

## 4 Results

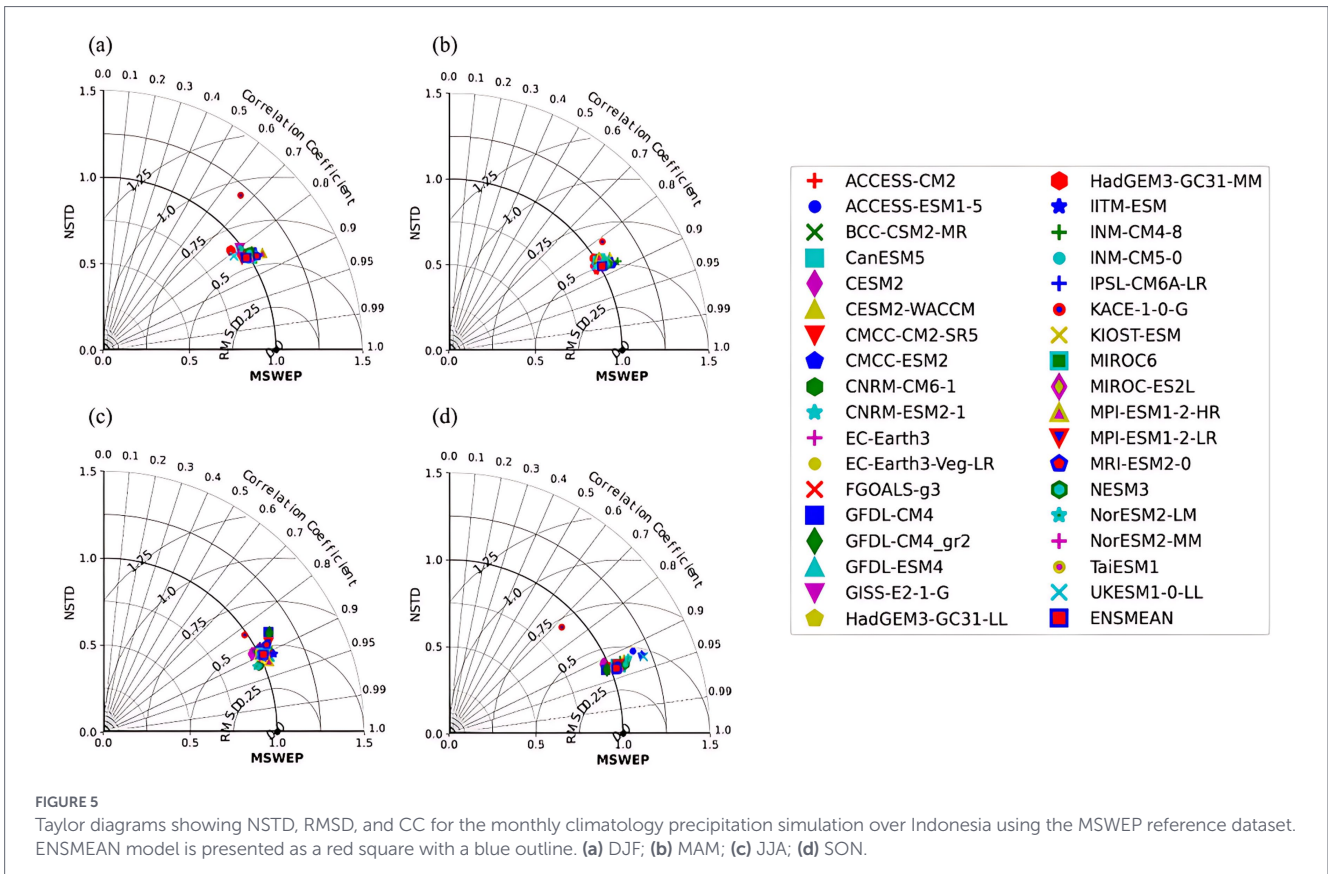
### 4.1 Model performance

The monthly precipitation cycles of 35 NEX-GDDP-CMIP6 and ENSMEAN models were compared with the reference dataset for 1985–2014 in Figure 3. The pink shades indicate the inter-model distribution, the wider bands represent higher uncertainty, and narrower bands signal stronger agreement. MSWEP annual variability as observed in the maximum precipitation of ~280–300 mm in January–March, minimum in July–August at ~150–170 mm, and an increase in September–December with ~280 mm. The figure showed that NorESM2-LM and MPI-ESM1-2-LR consistently overestimated the rainy season with the peaks reaching 320 mm in January–March to suggest a monsoonal pattern of precipitation. Meanwhile, CMCC-CM2-SR5 and MIROC6 indicated underestimated values in the dry season (JJA) below 150 mm. Thus, reflected the existence of dryness over the months. CanESM5, CESM2, and HadGEM3-GC31-LL exhibited values closer to MSWEP by maintaining seasonal amplitudes that were consistent with the observation data. BCC-CSM2-MR and GFDL-CM4 reproduced the seasonal shape but showed stronger deviations in April–May and October when precipitation tended to shift between rainy and dry seasons.

A critical observation in the annual cycle in Figure 3 is the consistent relative minimum in precipitation during February across most models, referred to as the ‘February dip’. This represents a systematic discrepancy, as the MSWEP reference dataset depicts a continuous peak during DJF. This model behavior likely stems from common biases in simulating the peak intensity of monsoonal flow in DJF. This underestimation reflects the challenge of simulating convection over the Indonesia complex topography (Peatman et al., 2014). The discrepancies also attributed to the model’s challenges in simulating large-scale monsoon circulation, land-sea contrast interactions and complex tropical dynamics (Mulsandi et al., 2024). Notably, the reference data of MSWEP documented to cause and underestimation of peak precipitation values (Beck et al., 2017).

The bias spread in the Taylor diagram compares the annual precipitation from NEX-GDDP-CMIP6 against the MSWEP. To reflect inter-model differences in seasonal precipitation, CC was scaled to range of 0–1. Visualization utilizes distinct symbols to represent individual models alongside the ENSMEAN. Figure 4 shows that majority of the models clustered close to the reference point. The CC scores exceeded 0.9 with low RMSD and the NSTD was close to one. The clusters showed that the models could replicate annual precipitation variability in Indonesia with reasonable accuracy. The best performance was determined based on the closeness of the scores to the reference point of MSWEP which included high CC, low RMSD, and near ideal NSTD. The results showed that ACCESS-CM2, CMCC-ESM2, MRI-ESM2.0, TaiESM1, and ENSMEAN had good performance by having positions close to the MSWEP. Meanwhile, poor performance was associated with high disparities compared to the reference point, determined using NSTD far from 1, higher RMSD, or weaker correlation. While most models cluster closely to the MSWEP reference, certain models exhibit deviations in variability. Specifically, ACCESS-ESM1-5 and KACE-1-0-G emerge as outliers with NSTD values exceeding 1.25 and 1.20, respectively. This indicates an overestimation of the observed precipitation variability. In contrast, GFDL-CM4 demonstrate high fidelity to observation, maintaining CC above 0.90 and an NSTD near unity.

The Taylor diagram for DJF, as shown in Figure 5a, demonstrated that most clusters of the models are close to the reference dataset. The CC score exceeding to 0.9, reflects the good performance in simulating seasonal precipitation variability during the period. ACCESS-CM2, CMCC-ESM2, MRI-ESM2.0, and ENSMEAN were in proximity to the reference point by showing high correlation, low RMSD, and NSTD close to one, suggested minimal bias in the intensity. The clustering pattern for MAM which is presented in Figure 5b is quite similar but the variances among all models become clearer. For example, TaiESM1, ACCESS-CM2, CMCC-ESM2, and ENSMEAN achieved CC scores close to 0.95–0.99 and recorded low RMSD. Thus, reflected the reliability of the models in reproducing precipitation variability and spatial distribution during the season.



In [Figure 5c](#), most models cluster near the observation point for JJA, showing high correlations ( $CC > 0.9$ ) and low RMSD. This indicated that most models effectively capturing dry season precipitation variability. ACCESS-CM2, CMCC-ESM2, TaiESM1, and ENSMEAN showed high correlation and minimal bias. The Taylor diagram for SON presented in [Figure 5d](#) shows that the models have greater spread compared to JJA. For example, ACCESS-CM2, CMCC-ESM2, MRI-ESM2.0, and ENSMEAN had high CC in the range of 0.95–0.99 and low RMSD, confirmed the model’s robustness in capturing seasonal precipitation patterns and distribution. KACE-1-0-G showed deviations in both NSTD and RMSD, reflected persistent deficiencies as previously observed in [Figures 5a–d](#).

### 4.2 Experiment ranking

The multi-criteria assessments are widely applied in climate science to identify the best GCMs to capture climate variabilities and patterns ([Nahar et al., 2017; Shakeel et al., 2025](#)). Section 3.3 provides information on the multi-criteria analysis to identify the models. [Figure 6](#) presents the heatmap ranking of the experiments. The scoring method adopted and described in Section 3.3 offered a comparative evaluation of climate models based on spatial and temporal performance. [Figure 6](#) shows the validity of the models in temporal and spatial dimensions with the warmer shades signaling a higher trend. The four columns on the left represent the normalized value of each evaluation metrics including  $r_{CC\_norm}$ ,  $r_{NSTD\_norm}$ ,  $r_{RMSD\_norm}$  and  $r_{MB\_norm}$  for the temporal dimension while the four on the right are for the spatial dimension. The row order is based on the ranking of the models. It was observed that ACCESS-CM2, CMCC-ESM2, TaiESM1, MRI-ESM2-0,

CESM2-WACCM and KIOST-ESM has high performance accuracy against the reference dataset.

ENSMEAN also showed high CC as identified in the warmer colors. The best models improved the representation of variability and reduction of errors to show superior reliability compared to the others. [The Figure 6](#) also shows the ability of the models in replicating spatial distribution of precipitation compared to temporal variability. The mean bias reflected the widest spread to emphasize the persistent errors due to overestimation and underestimation.

[Figure 7](#) depicts ACCESS-CM2 as the top-performing model across all dimensions. Even though trade-offs remained evident between temporal and spatial performance with some excelling in one dimension but weak in another. Temporal simulations measured the capacity of models to reproduce climate variability and long-term trends. The results showed that ACCESS-CM2, CMCC-ESM2, and MRI-ESM2.0 had good accuracy in replicating observed time series compared to the others. TaiESM1, KIOST-ESM, and CMCC-ESM2 also had the best performance in terms of spatial accuracy. Additionally, ACCESS-CM2 and CMCC-ESM2 emerged as the top-performing models in the composite evaluation of spatial and temporal performance, followed closely by TaiESM1 and MRI-ESM2.0. The evaluation ranked ACCESS-CM2, CMCC-ESM2, TaiESM1, MRI-ESM2.0, and CESM2-WACCM as the top five models, followed by KIOST-ESM in sixth and ENSMEAN in seventh.

### 4.3 Ability of the models to visualize Indonesia climatic pattern

The spatial distributions of the best ranking models including MSWEP, ACCESS-CM2 and ENSMEAN are compared in [Figure 8](#).

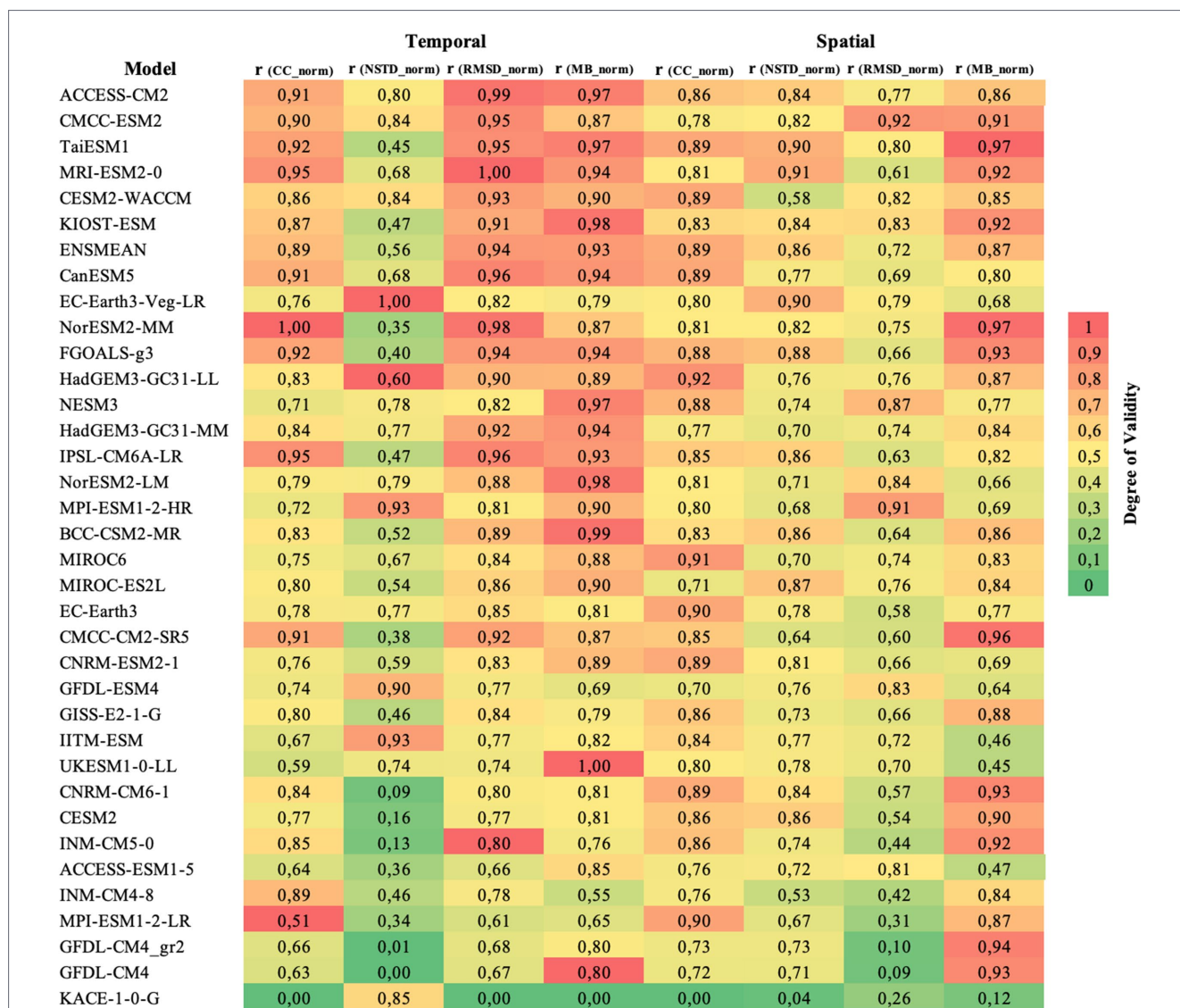


FIGURE 6 The heatmap of 35 NEX-GDDP-CMIP6 and ENSMEAN based on normalized evaluation metric scores such as r (CC\_norm), r (NSTD\_norm), r (RMSD\_norm) and r (MB\_norm) in simulating monthly precipitation. The columns represent spatial and temporal dimensions while the rows are the models. The order is the performance ranking with the best in the top 5 rows. The color represents the degree of validity with the green box showing poor connection while the red box signals near-perfect agreement with the reference dataset.

It was observed that the highest value of precipitation intensity during DJF exceeded 600 mm/month over some areas of Papua. ACCESS-CM2 exhibit better spatial performance than ENSMEAN during the season by providing closer spatial agreement to MSWEP as presented in heatmap (Figure 6). As shown in Figure 8, ACCESS-CM2 and ENSMEAN demonstrated comparable spatial performance over western and northern Indonesia, that captured the eastward expansion of wet condition during SON. ACCESS-CM2 also captured a reduction in precipitation magnitude over Sumatra, Java and Nusa Tenggara during MAM, compared to MSWEP. The same trend identified during JJA with magnitude less than 150 mm over Java, Nusa Tenggara, and southern Sumatra. Whereas ACCESS-CM2 exhibited slight overestimation in western Sumatra during JJA.

The temporal variation of precipitation across Indonesia can be classified into three climatic patterns of monsoonal, equatorial, and local (Aldrian and Dwi Susanto, 2003). Figure 9 compares monthly

mean precipitation for three representative regions which include Jakarta region for monsoonal, Pontianak region for equatorial, and Sorong region for local. While the models generally replicate the phase of Indonesia climatic types, systematic deviations from the MSWEP (red dashed line) persist throughout the annual cycle.

In Jakarta monsoonal regime, model trajectories deviate from MSWEP in almost every month. Thus, making a general characterization of “good match” difficult to maintain. During DJF wet season, ACCESS-CM2 and MRI-ESM2.0 exhibit magnitude deviations, underestimating peak precipitation. While during JJA dry months, MRI-ESM2-0 and CMCC-ESM2 appear visually closest to the MSWEP. Other models tend to overestimate dry season precipitation, suggesting a superior fit for specific models during this period compared to the higher uncertainty in transition months.

In the equatorial regime of Pontianak, all models captured the bimodal precipitation pattern, although quantitative deviations remain. ENSMEAN is closely in line with the MSWEP, reproducing

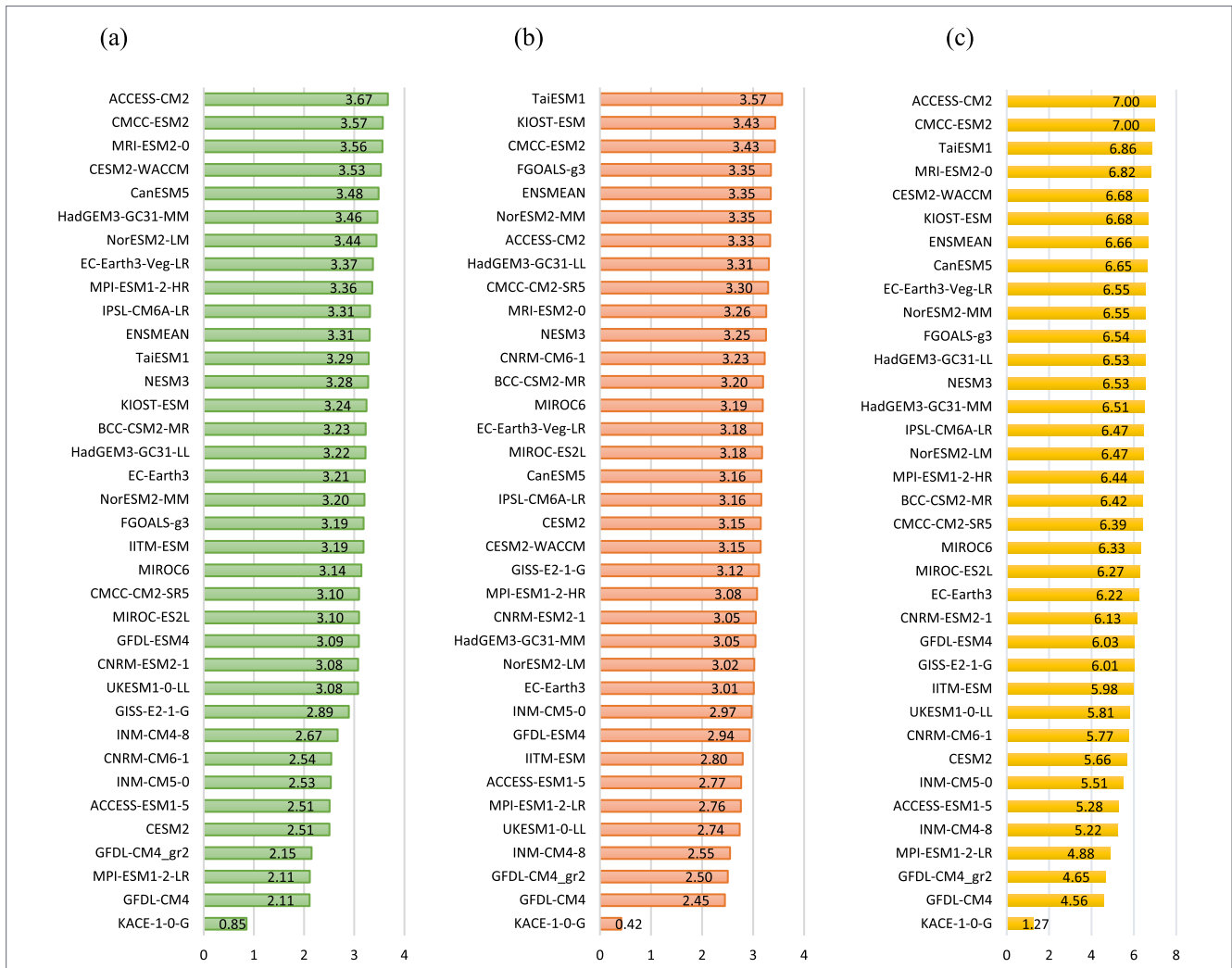


**FIGURE 7** Performance scores and ranking of 35 NEX-GDDP-CMIP6 models and the multi-model mean ensemble (ENSMEAN). Temporal-based and spatial-based normalized performance scores are shown in green and orange, respectively. The composite performance score (yellow) represents the unweighted sum of normalized spatio-temporal metrics, where higher values indicate better overall model performance. (a) Rank for temporal aspect. (b) Rank for spatial aspect. (c) Final rank of combined spatio-temporal aspect.

both intensity peaks with minimal bias. Compared to other individual simulations, ACCESS-CM2 captures the dual-peak structure but exhibits lower precipitation intensity than MSWEP. CMCC-ESM2 underestimates peak rainfall, while CESM2-WACCM shows a slight overestimation.

In Sorong local regime, precipitation variability is nearly uniform. Model fidelity shows marked variation peaking in JJA. During this period, MRI-ESM2-0 and CMCC-ESM2 appear most closely to the MSWEP. While ACCESS-CM2 and CESM2-WACCM show consistent monthly variation, CMCC-ESM2 exhibits a negative bias during the local rainy season. Although ENSMEAN follows the MSWEP pattern, inter-model differences in this region remain relatively small.

## 5 Discussion

Accurate long term global precipitation simulations are vital for assessing climate impacts and formulating adaptation strategies Vicente-Serrano et al. (2022). Many studies provided insights into the performance of GCMs in simulating precipitation. Raghavan et al. (2018)

reported the agreement of NEX-GDDP-CMIP6 with the observation over the historical period. Many studies focused in evaluating climate model (Singh et al., 2019; Taghavinia et al., 2023; Wu et al., 2020). However, these studies rarely identified single model with the best overall performance (Moradian et al., 2024). This is possibly due to the need for a comprehensive exploration of *in situ* observational data and region characteristic (Jain et al., 2019). There is also a need to adopt other methods to improve statistical performance (Wu et al., 2023). The reduction of uncertainty in the models is another important aspect, but the process can produce different results (Zhang et al., 2024).

Compared to previous research, this study provides new insight into NEX-GDDP-CMIP6 model assessments across Indonesia. This trend was confirmed by identifying the top five performing models: ACCESS-CM2, CMCC-ESM2, TaiESM1, MRI-ESM2-0, and CESM2-WACCM. ACCESS-CM2 showed statistical strength of high CC, lower error and near ideal NSTD as presented in Figure 6. This model also shows superior spatial representation over western and northern part of Indonesia as well as wet expansion in SON as depicted in Figure 8. ACCESS-CM2 had also been identified as the top 5 ranked model in similar studies conducted in Iran utilizing CMIP6 by Zabihi and Ahmadi (2024) and Ireland utilizing NEX-GDDP-CMIP6 by

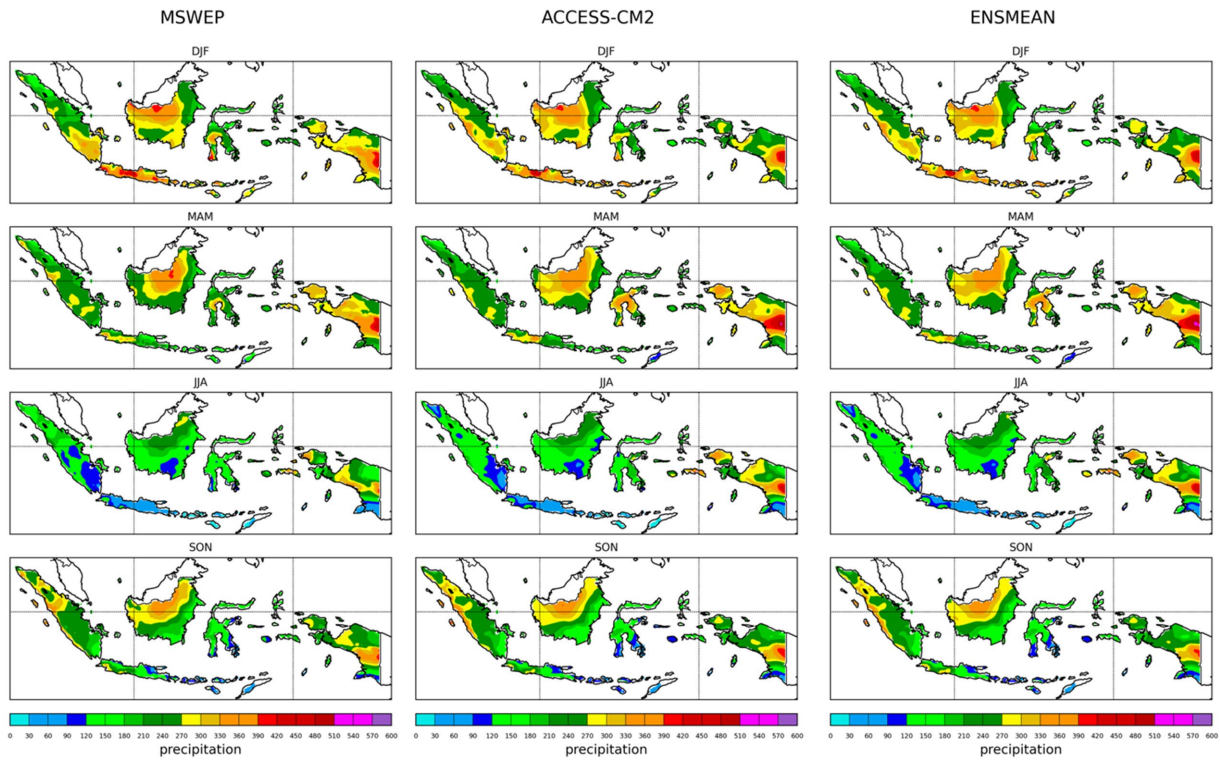


FIGURE 8 Spatial distribution plot of seasonal mean monthly precipitation measured at DJF, MAM, JJA, and SON to represent the MSWEP reference plot, the top-performing model ACCESS-CM2, and ENSMEAN model consecutively.

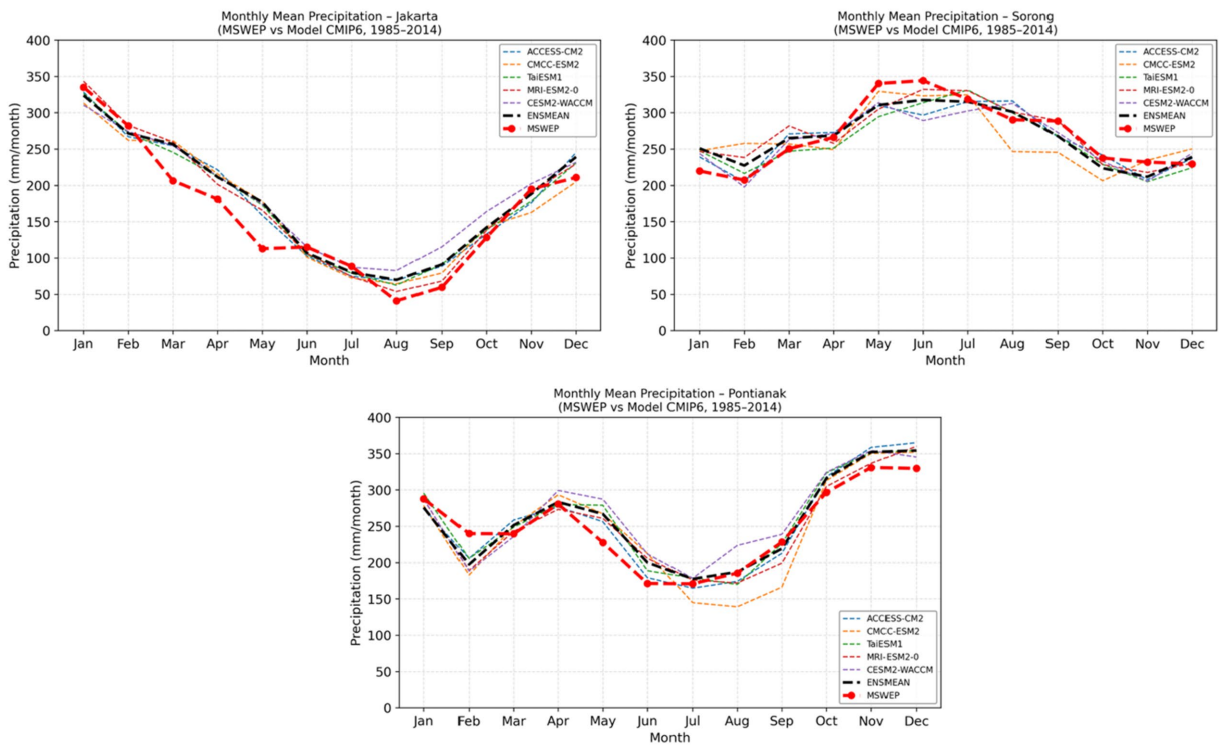


FIGURE 9 The monthly mean precipitation with the climatic patterns of Jakarta (monsoonal type), Pontianak (equatorial type), and Sorong (local type). The order of models in the legend corresponds to the rank while the red dashed line represents the reference dataset.

Moradian et al. (2024). ACCESS-CM2 demonstrate comparable spatial distribution with the observation over land (Figure 8) as reported by Bi et al., 2020. In Figure 7, CMCC-ESM2 exhibits strong spatio-temporal accuracy, consistent with its relatively low bias over Southeast Asia compared with other tropical regions in CMIP6 simulations (Lovato et al., 2022). As demonstrated in Figure 7, the TaiESM1 has the strongest spatial accuracy, this finding is related with the model's effectiveness in simulating monsoon-driven patterns (Wang et al., 2021). The statistical results shows that ACCESS-CM2 has the best temporal accuracy and the lowest error score as depicted in Figure 7. This aligns with finding by Gupta et al. (2025), that this model emerges as the top-ranked model overall in precipitation simulation. CESM2-WACCM indicated stronger temporal performance than spatial simulation in Figures 6, 7. The model also showed skill in simulating precipitation, with slight overestimation during JJA (Figure 9). Notably, CESM2-WACCM demonstrates superior ability to capture spatial precipitation trends over Uganda during SON compared with other CMIP6 models (Ngoma et al., 2021).

ENSMEAN in Figure 3 shows slight underestimation during the rainy season but exhibits strong performance during the dry season. The similar trend is identified in Taylor diagram (Figure 4), as reported also by Berhanu et al. (2025). The seasonal performance of ENSMEAN is reflected by its high CC of 0.8, a standard deviation close to 1, and the lowest error during the DJF wet season (Figure 5). ENSMEAN did not deviate significantly from the reference dataset and showed low bias during SON which marked the onset of pre-monsoon in Figure 3. The model also showed consistent skill in representing spatial patterns during dry season of MAM and JJA. ENSMEAN achieved better spatial performance as presented in Figure 6. It ranked seventh when the temporal and spatial dimensions were combined as depicted in Figure 7. In Figure 9, the models captured Indonesia three climatic regions, demonstrating added value of multi-model evaluation in enhancing confidence as well as reducing GCM uncertainty.

NEX-GDDP-CMIP6 performance over Indonesia Maritime Continent is related with how well the parent models resolve the region's climate engine mechanics or air-sea coupling (Zhang et al., 2023). A systematic bias remains where most models show underestimation in wet season of February (Figure 3). Suggests model's difficulties in simulating complex interaction between El Niño—Southern Oscillation (ENSO) and local orography over the maritime continent (Supari et al., 2018). Most models, including MSWEP reanalysis, struggle to accurately demonstrate precipitation during wet season in Figure 3. Whereas, during dry season, most models tend to overestimate the precipitation. These biases may drive by interactions between monsoons and local factors, such as orography and land-sea contrast, still challenge sub-grid parameterizations (Peatman et al., 2014). The proposed ranking method demonstrates it's ability to simulate precipitation across Indonesia's humid tropical monsoon region. This approach has also been successfully applied to semi-arid and arid regions, such as Morocco and Iran (Ayt Ougougdal et al., 2024; Zabihi and Ahmadi, 2024). This reinforces that model accuracy is highly region- dependent, although certain models exhibit consistent behavior across all climatic zones.

This study provided a benchmark for refining global and regional climate models through systematic assessment. The results serve as a reference for future CMIP6-based precipitation studies in tropical and monsoon-dominated regions. While this study provides valuable insights into the performance of NEX-GDDP-CMIP6 models across Indonesia, several limitations were identified. Firstly, although the current model's

evaluation utilizes historical monthly climatology for model selections, it is important to clarify that these findings are intended to support climate projections. Secondly, since the evaluation is based on mean monthly climatology, it does not account for interannual variability or extreme events simulations such as heavy precipitation or prolonged drought. Consequently, future study should incorporate annual and seasonal time-series metrics along with the standard extreme precipitation indices. Such addition will provide a more robust GCM's evaluation and better frame their application for Indonesia's climate regimes.

## 6 Conclusion

This study identified the five top-performing NEX-GDDP-CMIP6 models in simulating monthly mean precipitation across Indonesia. Model performance was evaluated against observation using metrics of CC, NSTD, RMSD and MB. Taylor diagram utilized to visualized model accuracy. By applying Min-Max normalization and the Summation of Rank method, this study compared individual models along with ENSMEAN across spatio-temporal scales using equal weighting.

In this study, no single model consistently outperformed the others across all evaluation criteria. Consequently, the proposed method was applied to enable a uniform and comprehensive evaluation. Statistical results indicate that ACCESS-CM2, CMCC-ESM2, and MRI-ESM2-0 provides the highest performance in simulating annual precipitation over temporal dimension. While TaiESM1, KIOST-ESM and CMCC-ESM2 exhibited better skill in seasonal precipitation across the spatial dimension. Overall, the five top-ranked models for simulating monthly climatological precipitation were identified as ACCESS-CM2, CMCC-ESM2, TaiESM1, MRI-ESM2-0, and CESM2-WACCM. Furthermore, ENSMEAN exhibited strong spatial agreement with MSWEP across Indonesia. Collectively, these models able to reproduce the three distinct climatic regions of Indonesia. This finding highlights the critical role of multi-model ensembles in mitigating individual GCM uncertainties and enhancing the reliability of regional climate projections. This study is particularly beneficial for climate impact assessments and water resource planning in tropical and monsoon-dominated regions.

Despite its benefits, debates continue regarding the selection of validation metrics for evaluating GCMs. Therefore, continued exploration is necessary to better align specific validation metrics with the intended purpose of the GCM's ranking. The existing GCM's has difficulties in accurately simulating precipitation dynamics due to climate engine over Indonesia Maritime Continent. These results should encourage further research into developing suitable models for the region, particularly in capturing extreme precipitation events. This information is vital for sectors such as water resources, ecosystems, and agriculture as well as decision-making and climate change mitigation strategies. Moreover, future research should incorporate climate scenarios using future datasets. Projection accuracy needs to be assessed for extreme precipitation events as well as other key climate parameters. Given the limited spatial coverage of surface observations in Indonesia, there is a significant opportunity to adopt blended satellite and in-situ dataset for improved representations.

A key limitation of this evaluation, which focuses on long-term monthly climatology, is that it does not directly assess the model's skill in simulating interannual variability (year-to-year fluctuations) or extreme events (such as heavy precipitation or prolonged drought).

## Data availability statement

The datasets analyzed in this study are publicly available. The NEX-GDDP-CMIP6 dataset was retrieved from the NASA Center for Climate Simulation (NCCS) (Thrasher et al., 2022; <https://doi.org/10.1038/s41597-022-01393-4>). Multi-Source Weighted-Ensemble Precipitation (MSWEP) data are described in Beck et al. (2019) and can be accessed via <https://doi.org/10.1175/BAMS-D-17-0138.1>.

## Author contributions

RP: Conceptualization, Data curation, Formal analysis, Methodology, Visualization, Validation, Writing – original draft, Writing – review & editing. AHS: Formal analysis, Investigation, Project administration, Supervision, Validation, Writing – review & editing. DD: Supervision, Data curation, Validation, Writing – review & editing. DSP: Conceptualization, Formal Analysis, Resources, Supervision, Validation, Writing – review & editing.

## Funding

The author(s) declared that financial support was received for this work and/or its publication. The authors express gratitude for the research grant provided for this study by the Centre for Human Resources and Development, the Agency for Meteorology, Climatology and Geophysics, Indonesia.

## Acknowledgments

This manuscript contains material from a dissertation by RP as part of the fulfillment of obtaining a Doctoral Degree at the Physics

## References

- Achutarao, K., Covey, C., Doutriaux, C., Fiorino, M., Gleckler, P., Phillips, T., et al. (2004). An appraisal of coupled climate model simulations. (Livermore, CA, USA: Program for Climate Model Diagnosis & Intercomparison (PCMDI)).
- Adriat, R., Aprilina, A., Satyawardhana, H., Ihwan, A., and Sutanto, Y. (2025). Identification of variations in the onset of the rainy and dry seasons in Indonesia. *J. Biosour. Environ. Sci.* 4, 102–111. doi: 10.61435/jbes.2025.19960
- Aldrian, E., and Dwi Susanto, R. (2003). Identification of three dominant rainfall regions within Indonesia and their relationship to sea surface temperature. *Int. J. Climatol.* 23, 1435–1452. doi: 10.1002/joc.950
- Ayt Ougougdal, H., Bounoua, L., Ech-chatir, L., and Yacoubi-Khebiza, M. (2024). Evaluation of the performance of CMIP6 models in simulating precipitation over Morocco. *Mediterr. Geosci. Rev.* 6, 145–158. doi: 10.1007/s42990-024-00121-x
- Baghel, T., Babel, M. S., Shrestha, S., Salin, K. R., Viridis, S. G. P., and Shinde, V. R. (2022). A generalized methodology for ranking climate models based on climate indices for sector-specific studies: an application to the Mekong sub-basin. *Sci. Total Environ.* 829. doi: 10.1016/j.scitotenv.2022.154551
- Bao, Y., and Wen, X. (2017). Projection of China's near- and long-term climate in a new high-resolution daily downscaled dataset NEX-GDDP. *J. meteorol. Res.* 31, 236–249. doi: 10.1007/s13351-017-6106-6
- Beck, H. E., Vergopolan, N., Pan, M., Levizzani, V., Van Dijk, A. I. J. M., Weedon, G. P., et al. (2017). Global-scale evaluation of 22 precipitation datasets using gauge observations

and hydrological modeling. *Hydrol. Earth Syst. Sci.* 21, 6201–6217. doi: 10.5194/hess-21-6201-2017

Beck, H. E., Wood, E. F., Pan, M., Fisher, C. K., Miralles, D. G., Van Dijk, A. I. J. M., et al. (2019). MSWep v2 global 3-hourly 0.1° precipitation: methodology and quantitative assessment. *Bull. Am. Meteorol. Soc.* 100, 473–500. doi: 10.1175/BAMS-D-17-0138.1

Berhanu, D., Alamirew, T., Bewket, W., Tarkegn, T. G., Zeleke, G., Hailelassie, A., et al. (2025). Evaluation of CMIP6 models in simulating seasonal extreme precipitation over Ethiopia. *Weather Clim. Extremes* 47. doi: 10.1016/j.wace.2025.100752

Bi, D., Dix, M., Marsland, S., O'farrell, S., Sullivan, A., Bodman, R., et al. (2020). Configuration and spin-up of ACCESS-CM2, the new generation Australian community climate and earth system simulator coupled model. *J. South. Hemisph. Earth Syst. Sci.* 70, 225–251. doi: 10.1071/ES19040

Boucher, O., Servonnat, J., Albright, A. L., Aumont, O., Balkanski, Y., Bastrikov, V., et al. (2020). Presentation and evaluation of the IPSL-CM6A-LR climate model. *J. Adv. Model. Earth Syst.* 12. doi: 10.1029/2019MS002010

Cao, J., Wang, B., Yang, Y. M., Ma, L., Li, J., Sun, B., et al. (2018). The NUIST earth system model (NESM) version 3: description and preliminary evaluation. *Geosci. Model Dev.* 11, 2975–2993. doi: 10.5194/gmd-11-2975-2018

Chang, C.-P., Ju, J., and Li, T. (2004) On the relationship between Western maritime continent monsoon rainfall and ENSO during northern Winter. (Boston, MA, USA:

## Conflict of interest

The author(s) declared that this work was conducted in the absence of any commercial or financial relationships that could be construed as a potential conflict of interest.

## Generative AI statement

The author(s) declared that Generative AI was not used in the creation of this manuscript.

Any alternative text (alt text) provided alongside figures in this article has been generated by Frontiers with the support of artificial intelligence and reasonable efforts have been made to ensure accuracy, including review by the authors wherever possible. If you identify any issues, please contact us.

## Publisher's note

All claims expressed in this article are solely those of the authors and do not necessarily represent those of their affiliated organizations, or those of the publisher, the editors and the reviewers. Any product that may be evaluated in this article, or claim that may be made by its manufacturer, is not guaranteed or endorsed by the publisher.

- American Meteorological Society (AMS)). Available online at: [https://doi.org/10.1175/1520-0442\(2004\)017%3C0665:OTRBWM%3E2.0.CO;2](https://doi.org/10.1175/1520-0442(2004)017%3C0665:OTRBWM%3E2.0.CO;2) (Accessed June 3, 2024).
- Chen, C. A., Hsu, H. H., and Liang, H. C. (2021). Evaluation and comparison of CMIP6 and CMIP5 model performance in simulating the seasonal extreme precipitation in the Western North Pacific and East Asia. *Weather Clim. Extrem.* 31. doi: 10.1016/j.wace.2021.100303
- Chen, W., Jiang, Z., and Li, L. (2011). Probabilistic Projections of Climate Change over China under the SRES A1B Scenario Using 28 AOGCMs. *Journal of Climate* 24, 4741–4756. doi: 10.1175/2011JCLI4102.1
- Cherchi, A., Fogli, P. G., Lovato, T., Peano, D., Iovino, D., Gualdi, S., et al. (2019). Global mean climate and main patterns of variability in the CMCC-CM2 coupled model. *J. Adv. Model. Earth Syst.* 11, 185–209. doi: 10.1029/2018MS001369
- Chhin, R., and Yoden, S. (2018). Ranking CMIP5 gcms for model ensemble selection on regional scale: case study of the indochina region. *JGR Atmosphere*. 123, 8949–8974. doi: 10.1029/2017JD028026
- Dahiya, K., Chilukoti, N., and Attada, R. (2024). Evaluating the climatic state of Indian summer monsoon during the mid-Pliocene period using CMIP6 model simulations. *Dyn. Atmos. Oceans* 106:101455. doi: 10.1016/j.dynatmoce.2024.101455
- Danabasoglu, G., Lamarque, J. F., Bacmeister, J., Bailey, D. A., DuVivier, A. K., Edwards, J., et al. (2020). The community earth system model version 2 (CESM2). *J. Adv. Model. Earth Syst.* 12. doi: 10.1029/2019MS001916
- Döscher, R., Acosta, M., Alessandri, A., Anthoni, P., Arsouze, T., Bergman, T., et al. (2022). The EC-Earth3 earth system model for the coupled model intercomparison project 6. *Geosci. Model Dev.* 15, 2973–3020. doi: 10.5194/gmd-15-2973-2022
- Dunne, J. P., Horowitz, L. W., Adcroft, A. J., Ginoux, P., Held, I. M., John, J. G., et al. (2020). The GFDL earth system model version 4.1 (GFDL-ESM 4.1): overall coupled model description and simulation characteristics. *J. Adv. Model. Earth Syst.* 12. doi: 10.1029/2019MS002015
- Ferijal, T., Mechram, S., Fauzi, A., and Ferdiansyah, T. (2025). Performance analysis of satellite-derived precipitation data in Aceh, Indonesia. *Int. J. Geoinform.* 21, 1–15. doi: 10.52939/ijg.v21i7.4311
- Francisco, R. V., Argete, J., Giorgi, F., Pal, J., Bi, X., and Gutowski, W. J. (2006). Regional model simulation of summer rainfall over the Philippines: effect of choice of driving fields and ocean flux schemes. *Theor. Appl. Climatol.* 86, 215–227. doi: 10.1007/s00704-005-0216-2
- Gates, W. L., Boyle, J. S., Covey, C., Dease, C. G., Doutriaux, C. M., Drach, R. S., et al. (1999). An overview of the results of the atmospheric model TM intercomparison project (AMIP I). (Boston, MA, USA: American Meteorological Society (AMS)). Available online at: [https://doi.org/10.1175/1520-0477\(1999\)080%3C0029:AOTR%3E2.0.CO;2](https://doi.org/10.1175/1520-0477(1999)080%3C0029:AOTR%3E2.0.CO;2) (Accessed March 19, 2024).
- Griffiths, M. L., Drysdale, R. N., Gagan, M. K., Zhao, J. x., Hellstrom, J. C., Ayliffe, L. K., et al. (2013). Abrupt increase in east Indonesian rainfall from flooding of the Sunda shelf ~9500 years ago. *Quat. Sci. Rev.* 74, 273–279. doi: 10.1016/j.quascirev.2012.07.006
- Gummadi, S., Samineni, S., and Lopez-Lavalle, L. A. B. (2025). Assessing high-resolution precipitation extremes in Central Asia: evaluation and future projections. *Clim. Chang.* 178. doi: 10.1007/s10584-025-03872-0
- Guo, J., Shen, Y., Wang, X., Liang, X., Liu, Z., and Liu, L. (2023). Evaluation and projection of precipitation extremes under 1.5°C and 2.0°C GWLs over China using bias-corrected CMIP6 models. *IScience* 26. doi: 10.1016/j.isci.2023.106179
- Gupta, R., Prakash, P., and Chembolu, V. (2025). Multi criteria evaluation of downscaled CMIP6 models in predicting precipitation extremes. *Atmospheric Research*. 315. doi: 10.1016/j.atmosres.2025.107921
- Hajima, T., Watanabe, M., Yamamoto, A., Tatebe, H., Noguchi, M. A., Abe, M., et al. (2020). Development of the MIROC-ES2L earth system model and the evaluation of biogeochemical processes and feedbacks. *Geosci. Model Dev.* 13, 2197–2244. doi: 10.5194/gmd-13-2197-2020
- Held, I. M., Guo, H., Adcroft, A., Dunne, J. P., Horowitz, L. W., Krasting, J., et al. (2019). Structure and performance of GFDL-ESM2.0 climate model. *J. Adv. Model. Earth Syst.* 11, 3691–3727. doi: 10.1029/2019MS001829
- Iqbal, Z., Shahid, S., Ahmed, K., Ismail, T., Khan, N., Virk, Z. T., et al. (2020). Evaluation of global climate models for precipitation projection in sub-Himalaya region of Pakistan. *Atmos. Res.* 245. doi: 10.1016/j.atmosres.2020.105061
- Iradukunda, P., Mwanauo, E. M., and Kabika, J. (2024). Modelling the future climate impacts on hydraulic infrastructure development in tropical (peri-)urban region: case of Kigali, Rwanda. *Heliyon* 10:e27126. doi: 10.1016/j.heliyon.2024.e27126
- Irwindi, H., Rosid, M. S., and Mart, T. (2021). The effects of ENSO, climate change and human activities on the water level of Lake Toba, Indonesia: a critical literature review. *Geosci. Lett.* 8. doi: 10.1186/s40562-021-00191-x
- Jain, S., Salunke, P., Mishra, S. K., Sahany, S., and Choudhary, N. (2019). Advantage of NEX-GDDP over CMIP5 and CORDEX data: Indian summer monsoon. *Atmos. Res.* 228, 152–160. doi: 10.1016/j.atmosres.2019.05.026
- Jiang, F., Wen, S., Gao, M., and Zhu, A. (2023). Assessment of NEX-GDDP-CMIP6 downscale data in simulating extreme precipitation over the Huai River basin. *Atmos.* 14. doi: 10.3390/atmos14101497
- Jun-Ichi, H., Yamanaka, M. D., Matsumoto, J., Agus WINARSO, P., and Sribimawati, T. (2002). Spatial and temporal variations of the rainy season over Indonesia and their link to ENSO. *J. meteorol. Soc. Japan* 80, 285–310. doi: 10.2151/jmsj.80.285
- Kelley, M., Schmidt, G. A., Nazarenko, L. S., Bauer, S. E., Ruedy, R., Russell, G. L., et al. (2020). GISS-E2.1: configurations and climatology. *J. Adv. Model. Earth Syst.* 12. doi: 10.1029/2019MS002025
- Konda, G., and Vissa, N. K. (2022). Robustness of BSISO and air-sea interactions in the CMIP (Phase-6) models over the North Indian Ocean. *Dyn. Atmos. Oceans* 99. doi: 10.1016/j.dynatmoce.2022.101316
- Kuhlbrodt, T., Jones, C. G., Sellar, A., Storkey, D., Blockley, E., Stringer, M., et al. (2018). The low-resolution version of HadGEM3 GC3.1: development and evaluation for global climate. *J. Adv. Model. Earth Syst.* 10, 2865–2888. doi: 10.1029/2018MS001370
- Kumar, P., Kumar, S., Barat, A., Sarthi, P. P., and Sinha, A. K. (2020). Evaluation of NASA'S NEX-GDDP-simulated summer monsoon rainfall over homogeneous monsoon regions of India. *Theor. Appl. Climatol.* 141, 525–536. doi: 10.1007/s00704-020-03188-2
- Kurniadi, A., Weller, E., Kim, Y. H., and Min, S. K. (2023). Evaluation of coupled model intercomparison project phase 6 model-simulated extreme precipitation over Indonesia. *Int. J. Climatol.* 43, 174–196. doi: 10.1002/joc.7744
- Lakew, H. B. (2020). Investigating the effectiveness of bias correction and merging MSWEP with gauged rainfall for the hydrological simulation of the upper Blue Nile basin. *J. Hydrol. Reg. Stud.* 32. doi: 10.1016/j.ejrh.2020.100741
- Lee, H. S. (2015). General rainfall patterns in Indonesia and the potential impacts of local seas on rainfall intensity. *Water* 7, 1751–1768. doi: 10.3390/w7041751
- Lee, H., Goodman, A., McGibbney, L., Waliser, D. E., Kim, J., Loikikh, P. C., et al. (2018). Regional climate model evaluation system powered by Apache open climate workbench v1.3.0: an enabling tool for facilitating regional climate studies. *Geosci. Model Dev.* 11, 4435–4449. doi: 10.5194/gmd-11-4435-2018
- Lee, T., Waliser, D. E., Li, J. L. F., Landerer, F. W., and Gierach, M. M. (2013). Evaluation of CMIP3 and CMIP5 wind stress climatology using satellite measurements and atmospheric reanalysis products. *J. Clim.* 26, 5810–5826. doi: 10.1175/JCLI-D-12-00591.1
- Liu, S., Raghavan, S. V., Ona, B. J., and Nguyen, N. S. (2023). Bias evaluation in rainfall over Southeast Asia in CMIP6 models. *J. Hydrol.* 621. doi: 10.1016/j.jhydrol.2023.129593
- Liu, T., Zhu, X., Tang, M., Guo, C., and Lu, D. (2024). Multi-model ensemble bias-corrected precipitation dataset and its application in identification of drought-flood abrupt alternation in China. *Atmos. Res.* 307. doi: 10.1016/j.atmosres.2024.107481
- Lovato, T., Peano, D., Butenschön, M., Matera, S., Iovino, D., Scoccimarro, E., et al. (2022). CMIP6 simulations with the CMCC earth system model (CMCC-ESM2). *J. Adv. Model. Earth Syst.* 14. doi: 10.1029/2021MS002814
- Lubis, S. W., Hagos, S., Hermawan, E., Respati, M. R., Ridho, A., Risyanto, et al. (2022). Record-breaking precipitation in Indonesia's capital of Jakarta in early January 2020 linked to the northerly surge, equatorial waves, and MJO. *Geophys. Res. Lett.* 49. doi: 10.1029/2022GL101513
- Lungarska, A., and Chakir, R. (2024). Projections of climate change impacts on ecosystem services and the role of land use adaptation in France. *Environ. Sustain. Indic.* 22:100369. doi: 10.1016/j.indic.2024.100369
- Mahiru Rizal, A., Sari Ningsih, N., Sofian, I., Hanifah, F., and Hilmi, I. (2019). Preliminary study of wave energy resource assessment and its seasonal variation along the southern coasts of Java, Bali, and Nusa Tenggara waters. *J. Renew. Sustain. Energy* 11. doi: 10.1063/1.5034161
- Mauritsen, T., Bader, J., Becker, T., Behrens, J., Bittner, M., Brokopf, R., et al. (2019). Developments in the MPI-M earth system model version 1.2 (MPI-ESM1.2) and its response to increasing CO<sub>2</sub>. *J. Adv. Model. Earth Systems* 11, 998–1038. doi: 10.1029/2018MS001400
- Meehl, G. A., Covey, C., McAvaney, B., Latif, M., and Stouffer, R. J. (2004) Overview of the coupled model intercomparison project (CMIP). (Boston, MA, USA: American Meteorological Society (AMS)).
- Mohammed, J. A. (2025). Performance evaluation and ranking of CMIP6 global climate models over upper Blue Nile (abbay) basin of Ethiopia. *Nat. Hazards Res.* 5, 61–74. doi: 10.1016/j.nhres.2024.06.004
- Moradian, S., Coleman, L., Kazmierczak, B., and Olbert, A. I. (2024). How to choose the most proper representative climate model over a study region? A case study of precipitation simulations in Ireland with NEX-GDDP-CMIP6 data. *Water Resour. Manag.* 38, 215–234. doi: 10.1007/s11269-023-03665-z
- Moradian, S., Iglesias, G., Broderick, C., and Olbert, I. A. (2023). Assessing the impacts of climate change on precipitation through a hybrid method of machine learning and discrete wavelet transform techniques, case study: Cork, Ireland. *J. Hydrol. Reg. Stud.* 49. doi: 10.1016/j.ejrh.2023.101523
- Müller, W. A., Jungclaus, J. H., Mauritsen, T., Baehr, J., Bittner, M., Budich, R., et al. (2018). A higher-resolution version of the max Planck institute earth system model (MPI-ESM1.2-HR). *J. Adv. Model. Earth Syst.* 10, 1383–1413. doi: 10.1029/2017MS001217
- Mulsandi, A., Koesmaryono, Y., Hidayat, R., Faqih, A., and Sopaheluwakan, A. (2024). Detecting Indonesian monsoon signals and related features using space-time singular value decomposition (SVD). *Atmos.* 15:187. doi: 10.3390/atmos15020187
- Musie, M., Sen, S., and Srivastava, P. (2020). Application of CORDEX-AFRICA and NEX-GDDP datasets for hydrologic projections under climate change in Lake Ziway sub-basin, Ethiopia. *J. Hydrol. Reg. Stud.* 31. doi: 10.1016/j.ejrh.2020.100721

- Nahar, J., Johnson, F., and Sharma, A. (2017). A rank-based approach for correcting systematic biases in spatial disaggregation of coarse-scale climate simulations. *J. Hydrol.* 550, 716–725. doi: 10.1016/j.jhydrol.2017.05.045
- Nazarian, R. H., Brizuela, N. G., Matijevic, B. J., Vizzard, J. V., Agostino, C. P., and Lutsko, N. J. (2024). Projected changes in mean and extreme precipitation over northern Mexico. *J. Clim.* 37, 2405–2422. doi: 10.1175/JCLI-D-23-0390.1
- Ngai, S. T., Juneng, L., Tangang, F., Chung, J. X., Supari, S., Salimun, E., et al. (2022). Projected mean and extreme precipitation based on bias-corrected simulation outputs of CORDEX Southeast Asia. *Weather Clim. Extrem.* 37. doi: 10.1016/j.wace.2022.100484
- Ngo-Duc, T., Nguyen-Duy, T., Desmet, Q., Trinh-Tuan, L., Ramu, L., Cruz, F., et al. (2024). Performance ranking of multiple CORDEX-SEA sensitivity experiments: towards an optimum choice of physical schemes for RegCM over Southeast Asia. *Clim. Dyn.* 62, 8659–8673. doi: 10.1007/s00382-024-07353-5
- Ngoma, H., Wen, W., Ayugi, B., Babausmail, H., Karim, R., and Ongoma, V. (2021). Evaluation of precipitation simulations in CMIP6 models over Uganda. *Int. J. Climatol.* 41, 4743–4768. doi: 10.1002/joc.7098
- Nur'utami, M. N., and Hidayat, R. (2016). Influences of IOD and ENSO to Indonesian rainfall variability: role of atmosphere-ocean interaction in the Indo-pacific sector. *Procedia Environ. Sci.* 33, 196–203. doi: 10.1016/j.proenv.2016.03.070
- Nwokolo, S. C., Ogbulezie, J. C., and Ushie, O. J. (2023). A multi-model ensemble-based CMIP6 assessment of future solar radiation and PV potential under various climate warming scenarios. *Optik* 285. doi: 10.1016/j.ijleo.2023.170956
- Pak, G., Noh, Y., Lee, M. I., Yeh, S. W., Kim, D., Kim, S. Y., et al. (2021). Korea Institute of Ocean Science and Technology earth system model and its simulation characteristics. *Ocean Sci. J.* 56, 18–45. doi: 10.1007/s12601-021-00001-7
- Peatman, S. C., Matthews, A. J., and Stevens, D. P. (2014). Propagation of the Madden-Julian oscillation through the maritime continent and scale interaction with the diurnal cycle of precipitation. *Q. J. R. Meteorol. Soc.* 140, 814–825. doi: 10.1002/qj.2161
- Pereira, H., Picado, A., Sousa, M. C., Alvarez, I., and Dias, J. M. (2023). Evaluation of earth system models outputs over the continental Portuguese coast: a historical comparison between CMIP5 and CMIP6. *Ocean Model* 184. doi: 10.1016/j.ocemod.2023.102207
- Pu, Y., Liu, H., Yan, R., Yang, H., Xia, K., Li, Y., et al. (2020). CAS FGOALS-g3 model datasets for the CMIP6 scenario model intercomparison project (ScenarioMIP). *Adv. Atmos. Sci.* 37, 1081–1092. doi: 10.1007/s00376-020-2032-0
- Qian, J.-H. (2008). Why precipitation is mostly concentrated over islands in the maritime continent. *Journal of the Atmospheric Sciences* 65, 1428–1441. doi: 10.1175/2007JAS2422.1
- Raghavan, S. V., Hur, J., and Liong, S. Y. (2018). Evaluations of NASA NEX-GDDP data over Southeast Asia: present and future climates. *Clim. Chang.* 148, 503–518. doi: 10.1007/s10584-018-2213-3
- Ramage, C. S. (1971). *Monsoon Meteorology*. (New York, NY, USA: Academic Press).
- Robertson, A. W., Moron, V., Qian, J. H., Chang, C. P., Tangang, F., Aldrian, E., et al. (2011). “The maritime continent monsoon” in *Global monsoon system, the: Research and forecast, 2nd edition* (eds. C.-P. Chang, Y. Ding, N.-C. Lau, R. H. Johnson, B. Wang and T. Yasunari. (World Scientific Publishing Co), 85–98.
- Rupp, D. E., Abatzoglou, J. T., Hegewisch, K. C., and Mote, P. W. (2013). Evaluation of CMIP5 20th century climate simulations for the Pacific Northwest USA. *J. Geophys. Res. Atmos.* 118, 10,884–10,906. doi: 10.1002/jgrd.50843
- Sarala, R. (2024). Machine learning and spatio-temporal patterns in climate change. *J. Inf. Syst. Eng. Manag.* 2025. doi: 10.52783/jisem.v10i15s.2431
- Séférian, R., Nabat, P., Michou, M., Saint-Martin, D., Voldoire, A., Colin, J., et al. (2019). Evaluation of CNRM earth system model, CNRM-ESM2-1: role of earth system processes in present-day and future climate. *J. Adv. Model. Earth Syst.* 11, 4182–4227. doi: 10.1029/2019MS001791
- Seland, Ø., Bentsen, M., Olivie, D., Toniazzo, T., Gjermundsen, A., Graff, L. S., et al. (2020). Overview of the Norwegian earth system model (NorESM2) and key climate response of CMIP6 DECK, historical, and scenario simulations. *Geosci. Model Dev.* 13, 6165–6200. doi: 10.5194/gmd-13-6165-2020
- Sellar, A. A., Walton, J., Jones, C. G., Wood, R., Abraham, N. L., Andrejczuk, M., et al. (2020). Implementation of U.K. earth system models for CMIP6. *J. Adv. Model. Earth Syst.* 12. doi: 10.1029/2019MS001946
- Shakeel, M., Abbas, H., Ali, Z., Tariq, A., Almazroui, M., and Kader, S. (2025). A novel framework for future drought characterization under ranked-based subset selection and weighted aggregative multi-modal ensemble of global climate models. *J. Environ. Manag.* 392. doi: 10.1016/j.jenvman.2025.126692
- Simão, M. L., Videiro, P. M., Silva, P. B. A., de Freitas Assad, L. P., and Sagrilo, L. V. S. (2020). Application of Taylor diagram in the evaluation of joint environmental distributions' performances. *Mar. Syst. Ocean Technol.* 15, 151–159. doi: 10.1007/s40868-020-00081-5
- Singh, V., Jain, S. K., and Singh, P. K. (2019). Inter-comparisons and applicability of CMIP5 GCMs, RCMs and statistically downscaled NEX-GDDP based precipitation in India. *Sci. Total Environ.* 697. doi: 10.1016/j.scitotenv.2019.134163
- Soumya, M. (2025). Role of Indonesian throughflow on Indian Ocean warming pattern formation during the recent global warming hiatus in CMIP6 models. *Glob. Planet. Change* 253. doi: 10.1016/j.gloplacha.2025.104969
- Sudarman, G. G., Hadi, T. W., Ningsih, N. S., Sopaheluwakan, A., Syahputra, M. R., and Marpaung, F. (2024). Nonstationary changes in annual rainfall over Indonesia's maritime continent. *Adv. Meteorol.* 2024. doi: 10.1155/2024/9392844
- Supari, Tangang, F., Salimun, E., Aldrian, E., Sopaheluwakan, A., and Juneng, L. (2018). ENSO modulation of seasonal rainfall and extremes in Indonesia. *Clim. Dyn.* 51, 2559–2580. doi: 10.1007/s00382-017-4028-8
- Swart, N. C., Cole, J. N. S., Kharin, V. V., Lazare, M., Scinocca, J. F., Gillett, N. P., et al. (2019). The Canadian earth system model version 5 (CanESM5.0.3). *Geosci. Model Dev.* 12, 4823–4873. doi: 10.5194/gmd-12-4823-2019
- Taghavinia, F., Zeinali, B., and Roudbari, A. D. (2023). Validation of temperature and precipitation variables of CMIP5 models in Iran under CORDEX and NEX-GDDP projects. *Physic. Geography Res. Quarterly* 55, 111–132. doi: 10.22059/JPHGR.2023.358843.1007772
- Tang, Y., and Yu, B. (2008). MJO and its relationship to ENSO. *J. Geophys. Res. Atmos.* 113. doi: 10.1029/2007JD009230
- Tatebe, H., Ogura, T., Nitta, T., Komuro, Y., Ogochi, K., Takemura, T., et al. (2019). Description and basic evaluation of simulated mean state, internal variability, and climate sensitivity in MIROC6. *Geosci. Model Dev.* 12, 2727–2765. doi: 10.5194/gmd-12-2727-2019
- Taylor, K. E. (2001). Summarizing multiple aspects of model performance in a single diagram. *J. Geophys. Res. Atmos.* 106, 7183–7192. doi: 10.1029/2000JD900719
- Thrasher, B., Wang, W., Michaelis, A., Melton, F., Lee, T., and Nemani, R. (2022). NASA global daily downscaled projections, CMIP6. *Scientific Data* 9. doi: 10.1038/s41597-022-01393-4
- Vicente-Serrano, S. M., García-Herrera, R., Peña-Angulo, D., Tomas-Burguera, M., Dominguez-Castro, F., Noguera, I., et al. (2022). Do CMIP models capture long-term observed annual precipitation trends? *Clim. Dyn.* 58, 2825–2842. doi: 10.1007/s00382-021-06034-x
- Voldoire, A., Saint-Martin, D., Sénési, S., Decharme, B., Alias, A., Chevallier, M., et al. (2019). Evaluation of CMIP6 DECK experiments with CNRM-CM6-1. *J. Adv. Model. Earth Syst.* 11, 2177–2213. doi: 10.1029/2019MS001683
- Volodin, E., and Gritsun, A. (2018). Simulation of observed climate changes in 1850–2014 with climate model INM-CM5. *Earth Syst. Dynam.* 9, 1235–1242. doi: 10.5194/esd-9-1235-2018
- Volodin, E. M., Mortikov, E. V., Kostyrykin, S. V., Galin, V. Y., Lykosov, V. N., Gritsun, A. S., et al. (2018). Simulation of the modern climate using the INM-CM48 climate model. *Russ. J. Numer. Anal. Math. Model.* 33, 367–374. doi: 10.1515/rnam-2018-0032
- Wang, Y. C., Hsu, H. H., Chen, C. A., Tseng, W. L., Hsu, P. C., Lin, C. W., et al. (2021). Performance of the Taiwan earth system model in simulating climate variability compared with observations and CMIP6 model simulations. *J. Adv. Model. Earth Syst.* 13. doi: 10.1029/2020MS002353
- Wati, T., Hadi, T. W., Sopaheluwakan, A., and Hutasoit, L. M. (2022). Statistics of the performance of gridded precipitation datasets in Indonesia. *Adv. Meteorol.* 2022. doi: 10.1155/2022/7995761
- Wheeler, M. C., and McBride, J. L. (2007). “Australian-Indonesian monsoon” in *Intraseasonal variability in the Atmosphere-Ocean climate system* (eds. W. K. M. Lau and D. E. Waliser (Springer Berlin Heidelberg), 125–173.
- Wu, F., Jiao, D., Yang, X., Cui, Z., Zhang, H., and Wang, Y. (2023). Evaluation of NEX-GDDP-CMIP6 in simulation performance and drought capture utility over China – based on DISO. *Hydrol. Res.* 54, 703–721. doi: 10.2166/nh.2023.140
- Wu, T., Lu, Y., Fang, Y., Xin, X., Li, L., Li, W., et al. (2019). The Beijing climate center climate system model (BCC-CSM): the main progress from CMIP5 to CMIP6. *Geosci. Model Dev.* 12, 1573–1600. doi: 10.5194/gmd-12-1573-2019
- Wu, Y., Miao, C., Duan, Q., Shen, C., and Fan, X. (2020). Evaluation and projection of daily maximum and minimum temperatures over China using the high-resolution NEX-GDDP dataset. *Clim. Dyn.* 55, 2615–2629. doi: 10.1007/s00382-020-05404-1
- Yamanaka, M. D. (2016). Physical climatology of Indonesian maritime continent: an outline to comprehend observational studies. *Atmos. Res.* 178–179, 231–259. doi: 10.1016/j.atmosres.2016.03.017
- Yuan, H. H., Huang, J. B., Ning, L. K., Catu, F., Zhou, J. W., Qiao, C., et al. (2024). Evaluation of precipitation extremes over the Tibetan plateau using the NASA global daily downscaled datasets NEX-GDDP-CMIP6. *Adv. Clim. Chang. Res.* 14, 884–895. doi: 10.1016/j.accre.2023.12.001
- Yukimoto, S., Kawai, H., Koshiro, T., Oshima, N., Yoshida, K., Urakawa, S., et al. (2019). The meteorological research institute earth system model version 2.0, MRI-ESM2.0: description and basic evaluation of the physical component. *J. meteorol. Soc. Japan* 97, 931–965. doi: 10.2151/jmsj.2019-051
- Zabihi, O., and Ahmadi, A. (2024). Multi-criteria evaluation of CMIP6 precipitation and temperature simulations over Iran. *J. Hydrol. Reg. Stud.* 52. doi: 10.1016/j.ejrh.2024.101707
- Zhang, Q., Liu, B., Li, S., and Zhou, T. (2023). Understanding models' global sea surface temperature bias in mean state: from CMIP5 to CMIP6. *Geophys. Res. Lett.* 50. doi: 10.1029/2022GL100888
- Zhang, F., Wei, L., Li, Y., Tang, H., Zhang, T., and Yang, B. (2024). Evaluation and projection of extreme high temperature indices in southwestern China using NEX-GDDP-CMIP6. *J. meteor. Res.* 38, 88–107. doi: 10.1007/s13351-017-6106-6
- Ziehn, T., Chamberlain, M. A., Law, R. M., Lenton, A., Bodman, R. W., Dix, M., et al. (2020). The Australian earth system model: ACCESS-ESM1.5. *J. South. Hemisph. Earth Syst. Sci.* 70, 193–214. doi: 10.1071/ES19035